TABLE III. Reactivity Between VLPs and Hyperimmune Antisera as Determined by Antigen ELISA

VLPs (ng/mL)		Hyperimmune sera						
		GI/1 Seto	GI/3 645	GI/4 Chiba	GII/3 809	GII/5 754	GII/7 10–25	GII/12 Chitta
rSeto	40	**4.007**	0.075	0.063	0.011	0.010	0.012	0.011
	4	**1.430**	0.034	0.023	0.009	0.011	0.014	0.010
	0.4	0.192	0.028	0.023	0.009	0.010	0.013	0.011
	0	0.010	0.028	0.013	0.008	0.011	0.012	0.011
r645	40	0.173	**3.235**	0.047	0.009	0.014	0.010	0.020
	4	0.061	**0.893**	0.035	0.010	0.010	0.009	0.013
	0.4	0.023	0.114	0.010	0.009	0.011	0.010	0.013
	0	0.010	0.030	0.010	0.009	0.014	0.010	0.015
r Chiba	40	0.105	0.034	**4.259**	0.009	0.012	0.010	0.011
	4	0.048	0.029	**1.408**	0.010	0.011	0.013	0.010
	0.4	0.011	0.026	**0.209**	0.010	0.010	0.010	0.010
	0	0.011	0.026	0.026	0.009	0.011	0.010	0.010
r809	40	0.060	0.028	0.023	**3.650**	0.075	0.056	0.066
	4	0.018	0.031	0.010	**1.271**	0.029	0.023	0.024
	0.4	0.013	0.034	0.007	**0.209**	0.015	0.013	0.014
	0	0.012	0.032	0.010	0.008	0.012	0.010	0.016
r754	40	0.011	0.030	0.025	0.014	**3.994**	0.041	0.083
	4	0.010	0.028	0.024	0.010	**1.329**	0.020	0.039
	0.4	0.010	0.029	0.025	0.010	0.184	0.012	0.015
	0	0.011	0.031	0.025	0.009	0.011	0.010	0.016
r10–25	40	0.018	0.049	0.025	0.016	0.107	**4.326**	0.100
	4	0.015	0.048	0.027	0.011	0.049	**1.343**	0.058
	0.4	0.010	0.038	0.025	0.010	0.017	0.160	0.021
	0	0.010	0.037	0.027	0.010	0.010	0.011	0.010
r Chitta	40	0.014	0.034	0.030	0.011	0.061	0.019	**3.356**
	4	0.011	0.031	0.026	0.010	0.022	0.012	**0.819**
	0.4	0.013	0.032	0.025	0.009	0.013	0.012	0.124
	0	0.014	0.024	0.024	0.009	0.012	0.011	0.025

The reaction was considered to be positive when the difference between the OD_{450} values for the hyperimmune and preimmune sera was >0.15 and the ratio was >2. Positive reactions were shown in boldface.

TABLE IV. Detection of NoV Antigens in Fecal Specimens by Antigen ELISA

Fecal Samples	Hyperimmune sera							EM	RT-PCR	Genotype
	GI/1 Seto	GI/3 645	GI/4 Chiba	GII/3 809	GII/5 754	GII/7 10–25	GII/12 Chitta			
2000K-600	**1.921**[a]	0.052	0.028	0.015	0.013	0.016	0.014	N/A[b]	+	GI/1
98-MC3	**1.407**	0.155	0.060	0.023	0.017	0.018	0.018	+	+	GI/1
98-MC4	**0.596**	0.086	0.056	0.029	0.017	0.018	0.017	–	+	GI/1
2000K-514	**0.498**	**1.521**	0.035	0.029	0.015	0.017	0.017	+	+	GI/3
2000K-518	**0.225**	**0.597**	0.033	0.017	0.012	0.015	0.016	–	+	GI/3
Se1	**0.450**	**2.641**	0.029	0.016	0.012	0.015	0.015	N/A	+	GI/3
2000K-691	0.038	0.040	**0.446**	0.017	0.013	0.015	0.015	+	+	GI/4
2000K-694	**0.358**	0.080	**4.899**	0.049	0.016	0.016	0.017	+	+	GI/4
96-844	0.166	0.071	**2.171**	0.017	0.014	0.015	0.017	+	+	GI/4
98K-826	0.022	0.051	0.065	**1.369**	0.016	0.039	0.066	+	+	GII/3
98K-836	0.018	0.037	0.032	**1.296**	0.015	0.042	0.030	+	+	GII/3
98-249	0.016	0.063	0.030	**1.083**	0.020	0.043	0.034	+	+	GII/3
95-277	0.016	0.034	0.023	0.015	**1.696**	0.024	0.029	+	+	GII/5
00-683	0.011	0.036	0.031	0.090	**0.428**	0.012	0.018	+	+	GII/5
00-684	0.012	0.025	0.015	0.039	**2.994**	0.041	0.136	+	+	GII/5
S99-75	0.037	0.041	0.071	0.101	0.147	**0.426**	0.168	N/A	+	GII/7
S99-21	0.008	0.021	0.035	0.021	0.082	**1.712**	0.010	N/A	+	GII/7
98-41	0.021	0.035	0.031	0.023	0.013	0.028	**1.433**	+	+	GII/12
98-2345	0.019	0.037	0.026	0.020	0.013	0.023	**0.453**	+	+	GII/12
99-1007	0.021	0.055	0.036	0.130	0.014	0.031	**2.722**	+	+	GII/12

[a]The reaction was considered to be positive when the difference between the OD_{450} values for the hyperimmune and preimmune sera was >0.15 and the ratio was >2. Positive reactions were shown in boldface.
[b]Not applicable.

antigen, although the titers were relatively low even in the homologous reaction. Another possible (even more likely) explanation is that the antigen ELISA is more sensitive than EM as described previously [Graham et al., 1994].

DISCUSSION

This study describes the cloning, sequencing, and expression of the capsid proteins of four currently circulating NoV strains and their genetic and antigenic relationships with three previously characterized strains. The phylogenetic analyses indicated that these seven strains belong to GI/1, GI/3, GI/4, GII/3, GII/5, GII/7, and GII/12. In contrast to the rapid accumulation of information for genetic diversity, at least 14 in the GI and 17 in the GII genotypes, studies on the determination of antigenic type have been relatively slow [Kageyama et al., 2004]. This is because generation of the VLPs antigen is not an easy task, and a comparative study with a panel of a large number of VLPs antigens and their antisera is difficult to be performed at the moment. Continued preparation and characterization of more VLPs antigens and their hyperimmune sera are highly useful to refine the panel.

Although the seven antigenic types were distinguishable by the hyperimmune antisera generated against the VLPs, low levels of cross-reaction were observed among these strains when the antibody ELISA was used. Because no NoV specific antibody was detected in the preimmune animal sera, the cross-reactive antibodies in the hyperimmune antisera originated from common antigenic epitopes among NoVs. In fact, Kitamoto et al. [2002] obtained not only genogroup-specific, but also common cross-reactive monoclonal antibodies (MAbs) for four GI and six GII VLPs. Further characterization of antigenic epitopes using MAbs for the antigenic type-specific diagnosis of NoV is needed. In antibody ELISA (Table II), higher responses were observed between the intra-genogroup strains than between the inter-genogroup strains. This observation is worth noting, because it indicates that GI and GII are not only genetically, but also antigenically distinct.

Previous observations of the immune responses of patients involved in outbreaks have also explained the common antigenic epitopes. Immune responses to multiple antigenic types, most of which were caused by a single NoV strain, are often detected in outbreaks of gastroenteritis [Vipond et al., 2004]. Higher responses to homotypic than to heterotypic strains may allow us to make a seroresponse-based diagnosis of NoV infection. Indeed, we recently identified a GII/4 infection in a hospital based on the immune responses of the patients (data not shown).

As has been shown in the case of the Norwalk virus, Mexico virus, Grimsby virus, Seto virus, Chiba virus, and Chitta virus, the antigen ELISA for NoV was highly genotype-specific [Numata et al., 1994; Hale et al., 1996, 1999; Kobayashi et al., 2000a,b,c]. Further generation of VLPs antigens and hyperimmune sera against each genotype VLPs and the subsequent development of both antibody and antigen ELISAs are necessary for the detection of NoVs, for the antigenic relationship among NoVs, and for the classification of NoVs.

ACKNOWLEDGMENTS

This work was supported in part by a grant for Research on Emerging and Re-emerging Infectious Diseases, a grant for Special Research, a grant for Research on Food Safety, and a grant for Research on Health Sciences focusing on Drug Innovation from the Ministry of Health, Labor, and Welfare of Japan.

REFERENCES

Atmar RL, Estes MK. 2001. Diagnosis of noncultivatable gastroenteritis viruses, the human caliciviruses. Clin Microbiol Rev 14: 15–37.

Belliot G, Noel JS, Li JF, Seto Y, Humphrey CD, Ando T, Glass RI, Monroe SS. 2001. Characterization of capsid genes, expressed in the baculovirus system, of three new genetically distinct strains of "Norwalk-like viruses." J Clin Microbiol 39:4288–4295.

Dingle KE, Lambden PR, Caul EO, Clarke IN. 1995. Human enteric Caliciviridae: The complete genome sequence and expression of virus-like particles from a genetic group II small round structured virus. J Gen Virol 76:2349–2355.

Duizer E, Schwab KJ, Neill FH, Atmar RL, Koopmans MP, Estes MK. 2004. Laboratory efforts to cultivate noroviruses. J Gen Virol 85:79–87.

Estes MK, Atmar RL, Hardy ME. 1997. Norwalk and related diarrhea viruses. In: Richmann DD, Whitley RJ, Hayden FG, editors. Clinical virology. New York: Churchill Livingstone, Inc. pp 1073–1095.

Feisenstein J. 1985. Confidence limits on phylogenies: An approach using the bootstrap. Evolution 39:783–791.

Glass PJ, White LJ, Ball JM, Leparc-Goffart I, Hardy ME, Estes MK. 2000. Norwalk virus open reading frame 3 encodes a minor structural protein. J Virol 74:6581–6591.

Graham DY, Jiang X, Tanaka T, Opekun AR, Madore HP, Estes MK. 1994. Norwalk virus infection of volunteers: New insights based on improved assays. J Infect Dis 170:34–43.

Gray JJ, Jiang X, Morgan-Capner P, Desselberger U, Estes MK. 1993. Prevalence of antibodies to Norwalk virus in England: Detection by enzyme-linked immunosorbent assay using baculovirus-expressed Norwalk virus capsid antigen. J Clin Microbiol 31:1022–1025.

Green KY, Lew JF, Jiang X, Kapikian AZ, Estes MK. 1993. Comparison of the reactivities of baculovirus-expressed recombinant Norwalk virus capsid antigen with those of the native Norwalk virus antigen in serologic assays and some epidemiologic observations. J Clin Microbiol 31:2185–2191.

Green SM, Lambden PR, Caul EO, Clarke IN. 1997. Capsid sequence diversity in small round structured viruses from recent UK outbreaks of gastroenteritis. J Med Virol 52:14–19.

Green KY, Ando T, Balayan MS, Clarke IN, Estes MK, Matson DO, Nakata S, Neill JD, Struddert MJ, J TH. 2001a. Caliciviridae. In: van Regenmortel MHV, Fauquet CM, Bishop DHL, Carsten EB, Estes MK, Lemon SM, Maniloff J, Maya MA, McGeoch DJ, Pringle CR, Wickner RB, editors. Virus taxonomy. 3rd edn, San Diego: Academic Press, Inc. pp 725–734.

Green KY, Chanock RM, Kapikian AZ. 2001b. Human caliciviruses. In: Knipe DM, Howley PM, Griffin DE, editors. Fields virology, 4th edn, Philadelphia: Lippincott Williams & Wilkins. pp 841–874.

Hale AD, Lewis D, Green J, Jiang X, Brown DWG. 1996. Evaluation of an antigen capture ELISA based on recombinant Mexico virus capsid protein. Clin Diagn Virol 5:27–35.

Hale AD, Crawford SE, Ciarlet M, Green J, Gallimore C, Brown DW, Jiang X, Estes MK. 1999. Expression and self-assembly of Grimsby virus: Antigenic distinction from Norwalk and Mexico viruses. Clin Diagn Lab Immunol 6:142–145.

Jiang X, Wang M, Graham DY, Estes MK. 1992. Expression, self-assembly, and antigenicity of the Norwalk virus capsid protein. J Virol 66:6527–6532.

Jiang X, Wang M, Wang K, Estes MK. 1993. Sequence and genomic organization of Norwalk virus. Virology 195:51–61.

Jiang X, Cubitt D, Hu J, Dai X, Treanor J, Matson DO, Pickering LK. 1995a. Development of an ELISA to detect MX virus, a human calicivirus in the snow mountain agent genogroup. J Gen Virol 76:2739–2747.

Jiang X, Matson DO, Ruiz-Palacios GM, Hu J, Treanor J, Pickering LK. 1995b. Expression, self-assembly, and antigenicity of a snow mountain agent-like calicivirus capsid protein. J Clin Microbiol 33:1452–1455.

Jiang X, Wang J, Estes MK. 1995c. Characterization of SRSVs using RT-PCR and a new antigen ELISA. Arch Virol 140:363–374.

Jiang X, Zhong WM, Farkas T, Huang PW, Wilton N, Barrett E, Fulton D, Morrow R, Matson DO. 2002. Baculovirus expression and antigenic characterization of the capsid proteins of three Norwalk-like viruses. Arch Virol 147:119–130.

Kageyama T, Shinohara M, Uchida K, Fukushi S, Hoshino FB, Kojima S, Takai R, Oka T, Takeda N, Katayama K. 2004. Co-existence of multiple genotypes, including newly identified genotypes, in outbreaks of Norovirus gastroenteritis. J Clin Microbiol 42:2988–2995.

Kapikian AZ. 1994. Norwalk and Norwalk-like viruses. In: Kapikian AZ, editor. Viral infections of the gastroentestinal tract. 2nd edn, New York: Marcel Dekker, Inc. pp 471–518.

Kapikian AZ, Estes MK, Chanock RM. 1996. Norwalk group of viruses. In: Fields BN, Knipe DM, Howley PM, Chanock RM, Melnick JL, Monath TP, Roizmann B, Straus SE, editors. Fields virology. 3rd edn, Philadelphia, PA: Lippincott–Raven Publishers. pp 783–810.

Katayama K, Shirato-Horikoshi H, Kojima S, Kageyama T, Oka T, Hoshino F, Fukushi S, Shinohara M, Uchida K, Suzuki Y, Gojobori T, Takeda N. 2002. Phylogenetic analysis of the complete genome of 18 Norwalk-like viruses. Virology 299:225–239.

Kimura M. 1980. A simple method for estimating evolutionary rates of base substitutions through comparative studies of nucleotide sequences. J Mol Evol 16:111–120.

Kitamoto N, Tanaka T, Natori K, Takeda N, Nakata S, Jiang X, Estes MK. 2002. Cross-reactivity among several recombinant calicivirus virus-like particles (VLPs) with monoclonal antibodies obtained from mice immunized orally with one type of VLP. J Clin Microbiol 40:2459–2465.

Kobayashi S, Sakae K, Natori K, Takeda N, Miyamura T, Suzuki Y. 2000a. Serotype-specific antigen ELISA for detection of Chiba virus in stools. J Med Virol 62:233–238.

Kobayashi S, Sakae K, Suzuki Y, Shinozaki K, Okada M, Ishiko H, Kamata K, Suzuki K, Natori K, Miyamura T, Takeda N. 2000b. Molecular cloning, expression, and antigenicity of Seto virus belonging to genogroup I Norwalk-like viruses. J Clin Microbiol 38:3492–3494.

Kobayashi S, Sakae K, Suzuki Y, Ishiko H, Kamata K, Suzuki K, Natori K, Miyamura T, Takeda N. 2000c. Expression of recombinant capsid proteins of chitta virus, a genogroup II Norwalk virus, and development of an ELISA to detect the viral antigen. Microbiol Immunol 44:687–693.

Kojima S, Kageyama T, Fukushi S, Hoshino FB, Shinohara M, Uchida K, Natori K, Takeda N, Katayama K. 2002. Genogroup-specific PCR primers for detection of Norwalk-like viruses. J Virol Methods 100:107–114.

Lambden PR, Caul EO, Ashley CR, Clarke IN. 1993. Sequence and genome organization of a human small round-structured (Norwalk-like) virus. Science 259:516–519.

Lew JF, Kapikian AZ, Jiang X, Estes MK, Green KY. 1994. Molecular characterization and expression of the capsid protein of a Norwalk-like virus recovered from a Desert Shield troop with gastroenteritis. Virology 200:319–325.

Lew JF, Kapikian AZ, Valdesuso J, Green KY. 1994. Molecular characterization of Hawaii virus and other Norwalk-like viruses: Evidence for genetic polymorphism among human caliciviruses. J Infect Dis 170:535–542.

Li TC, Yamakawa Y, Suzuki K, Tatsumi M, Razak MA, Uchida T, Takeda N, Miyamura T. 1997. Expression and self-assembly of empty virus-like particles of hepatitis E virus. J Virol 71:7207–7213.

Numata K, Nakata S, Jiang X, Estes MK, Chiba S. 1994. Epidemiological study of Norwalk virus infections in Japan and Southeast Asia by enzyme-linked immunosorbent assays with Norwalk virus capsid protein produced by the baculovirus expression system. J Clin Microbiol 32:121–126.

Parker S, Cubitt D, Jiang JX, Estes M. 1993. Efficacy of a recombinant Norwalk virus protein enzyme immunoassay for the diagnosis of infections with Norwalk virus and other human "candidate" caliciviruses. J Med Virol 41:179–184.

Parker SP, Cubitt WD, Jiang XJ, Estes MK. 1994. Seroprevalence studies using a recombinant Norwalk virus protein enzyme immunoassay. J Med Virol 42:146–150.

Parker SP, Cubitt WD, Jiang X. 1995. Enzyme immunoassay using baculovirus-expressed human calicivirus (Mexico) for the measurement of IgG responses and determining its seroprevalence in London, UK. J Med Virol 46:194–200.

Prasad BV, Rothnagel R, Jiang X, Estes MK. 1994. Three-dimensional structure of baculovirus-expressed Norwalk virus capsids. J Virol 68:5117–5125.

Prasad BV, Hardy ME, Dokland T, Bella J, Rossmann MG, Estes MK. 1999. X-ray crystallographic structure of the Norwalk virus capsid. Science 286:287–290.

Saitou N, Nei M. 1987. The neighbor-joining method: A new method for reconstructing phylogenetic trees. Mol Biol Evol 4:406–425.

Vipond IB, Caul EO, Hirst D, Carmen B, Curry A, Lopman BA, Pead P, Pickett MA, Lambden PR, Clarke IN. 2004. National epidemic of Lordsdale Norovirus in the UK. J Clin Virol 30:243–247.

JOURNAL OF CLINICAL MICROBIOLOGY, Sept. 2005, p. 4460–4465 Vol. 43, No. 9
0095-1137/05/$08.00+0 doi:10.1128/JCM.43.9.4460–4465.2005

Detection and Characterization of Human Group C Rotaviruses in Bangladesh

Mustafizur Rahman,[1,2]* Sukalyani Banik,[1] Abu S. G. Faruque,[1] Koki Taniguchi,[3] David A. Sack,[1] Marc Van Ranst,[2] and Tasnim Azim[1]

ICDDR,B, Centre for Health and Population Research, Mohakhali, Dhaka 1212, Bangladesh[1]; Laboratory of Clinical and Epidemiological Virology, Rega Institute for Medical Research, University of Leuven, B-3000, Leuven, Belgium[2]; and Department of Virology and Parasitology, Fujita Health University School of Medicine, Toyoake, Aichi 470-1192, Japan[3]

Received 7 January 2005/Returned for modification 28 May 2005/Accepted 25 June 2005

Group C rotaviruses were detected by reverse transcription-PCR in 14 (2.3%) of 611 group A rotavirus-negative stool specimens from the patients admitted to the International Centre for Diarrhoeal Disease Research, Bangladesh hospital, Dhaka, Bangladesh, during July to December 2003. The low rate of detection suggested that infection with group C rotaviruses was an uncommon cause of hospitalization due to gastroenteritis. In addition, coinfections with pathogenic enteric bacteria were frequently observed in group C rotavirus-infected patients. Nucleotide sequence comparison of the VP4, VP6, and VP7 genes revealed that the Bangladeshi group C rotaviruses were most similar to Nigerian group C rotavirus strains. Phylogenetic analysis suggested that all human group C rotaviruses, including the strains isolated in our study, clustered in a monophyletic branch, which was distantly related to the branch comprised of animal group C rotaviruses.

Rotaviruses are classified into seven antigenically distinct groups (A to G) on the basis of a common group antigen, the inner capsid protein (VP6). Groups A, B, and C are associated with acute gastroenteritis in humans and animals while groups D, E, F, and G only infect animals (11, 32, 33). In contrast to group A rotaviruses, which are the most common viral agents causing diarrheal infections in children younger than 3 years, group C rotaviruses cause sporadic cases of acute diarrhea or outbreaks of illness in children older than 3 years and adults (25, 27, 42). Seroepidemiological investigations have demonstrated that antibodies to group C rotaviruses are present in as much as 3 to 45% of the population tested. The viral detection rate in humans has remained low (5, 19, 30, 40). Therefore, the role of group C rotaviruses in the global picture of diarrheal illness has remained unresolved.

Group C rotaviruses were first isolated in piglets in 1980 (34) and in humans in 1982 (31). Since then, they have been recognized in humans and animals, both in industrialized countries including Australia, United States, United Kingdom, Finland, and Japan and in developing countries or regions such as India, China, Malaysia, and Latin America (3, 4, 5, 8, 10, 18, 22, 26, 29, 41). Thus, group C rotavirus strains are globally distributed and are thought to be one of the emerging pathogens in humans. However, no group C rotavirus infection either in animals or in humans has been reported from Bangladesh thus far.

Like group A rotaviruses, group C rotaviruses contain 11 segments of double-stranded RNA, but their RNA migration pattern in polyacrylamide gel electrophoresis (PAGE) is different (4-3-2-2) from that of group A rotaviruses (4-2-3-2). Serotyping of group C rotaviruses remains complicated due to the difficulties in adapting human group C rotaviruses in cell culture (13, 28). Sequence comparison suggests that genetic diversity exists among group C rotaviruses, although on a much narrower scale than among group A rotaviruses. Genotyping for group C rotaviruses has been proposed; however, no formal classification system based on VP4 (P type) and VP7 (G type) has been established (12, 16, 20, 39). Porcine Cowden and bovine Shintoku strains were proposed as different G serotypes, and the existence of a third G serotype for porcine HF strain was suggested (39). All human group C rotaviruses analyzed so far belong to a fourth G serotype, and a high degree of conservation exists among them (1, 6, 16, 21). Evolutionary studies also indicate that human group C rotaviruses evolved quite recently and possibly belong to a single globally distributed genotype (7, 16, 21). Jiang and colleagues (20) proposed three P genotypes, where human, porcine, and bovine group C rotaviruses constituted the different groups.

The International Centre for Diarrhoeal Disease Research, Bangladesh (ICDDR,B) hospital in Dhaka in central Bangladesh treats about 100,000 diarrheal patients a year. In a systematic surveillance system (37), stool samples are collected from 2% of the patients attending the hospital for laboratory determination of the presence of bacterial and viral enteric pathogens. As part of this surveillance study, we determined the prevalence of group C rotaviruses among hospitalized patients who were negative for group A rotaviruses. We sequenced the VP4, VP6, and VP7 genes of the local group C rotavirus strains. Their genetic relationship with other group C rotavirus strains circulating all over the world was also examined.

* Corresponding author. Mailing address: Senior Research Officer, Virology Laboratory, Laboratory Sciences Division, ICDDR,B, Centre for Health and Population Research, Mohakhali, Dhaka 1212, Bangladesh. Phone: 8802-8811751-60, ext. 2409. Fax: 8802-881-2529. E-mail: mustafizur.rahman@uz.kuleuven.ac.be.

MATERIALS AND METHODS

Study population and data collection. During July to December 2003, about 50,000 patients were admitted to the ICDDR,B Dhaka hospital with a history of watery diarrhea. As part of the surveillance, the stool specimens from every 50th

patient (2% of sample; $n = 956$) were tested for various common enteric pathogens, which included group A rotaviruses and *Vibrio*, *Shigella*, and *Salmonella* species. In the present study, the stool specimens negative for group A rotaviruses ($n = 611$) were tested for group C rotaviruses.

Pooling of the samples. To decrease the costs of testing we have performed a two-step testing procedure, whereby specimens were first tested in pools of 10 samples in a single test by reverse transcription-PCR (RT-PCR), followed by a second PCR. It was considered that all samples in the negative pools were negative. Samples from positive pools were retested individually to determine which sample in the pool was positive. Pooling of 10 samples with the expected prevalence of group C rotaviruses (1 to 5%) resulted in a reduction of 40 to 80% of the laboratory costs.

Electropherotyping. One-hundred microliters of 2% stool suspensions in phosphate-buffered saline was treated with sodium acetate and extracted with an equal volume of phenol:chloroform:isoamylalcohol (25:24:1) mixture. The extracted RNA was tested for electropherotype (E-type) by polyacrylamide gel electrophoresis (PAGE) as described by Herring et al. (17).

Reverse transcription-PCR. RNA was extracted from the stool suspension using the QIAamp Viral RNA mini kit (QIAGEN/Westburg, Leusden, The Netherlands) according to the manufacturer's instructions. RT-PCR was carried out using the OneStep RT-PCR kit (QIAGEN/Westburg). The primers specific for the group C rotavirus VP6 gene were used as described by Gouvea et al. (15). The reaction was carried out with an initial reverse transcription step at 45°C for 30 min, followed by 40 cycles of amplification (30 s at 94°C, 30 s at 50°C, 1 min at 72°C) and a final extension of 7 min at 72°C in a thermal cycler. PCR products were run on a 1.5% ethidium bromide-stained agarose gel and visualized under UV light. A specific segment size (356 bp) for a group C rotavirus DNA product was observed on stained gels. A second PCR was also carried out with the first PCR product as a template using the same primer pairs.

Nucleotide sequencing. The PCR amplicons were purified with the QIAquick PCR purification kit (QIAGEN/Westburg) and sequenced in both directions using the dideoxy nucleotide chain termination method with the ABI PRISM BigDye Terminator Cycle Sequencing Reaction kit (Perkin-Elmer Applied Biosystems, Foster City, Calif.) on an automated sequencer (ABI PRISM 310). The consensus primers GrC VP7-20F (5′-GCTGTCTGACAAACTGGTC-3′; strain Jajeri, accession number AF323982, nucleotide [nt] 20 to 38) and GrC VP7-1062R (5′-GCCACATGATCTTGTTTACGC-3′; strain Jajeri, nt 1042 to 1062) were used for VP7 gene sequencing. For the VP4 gene, consensus primers GrC VP4-1F (5′-GGCTTAAAAAGTAGAGATCG-3′; strain Jajeri, accession number AF323981, nt 1 to 20) and GrC VP4-1243R (5′-CCAGGATATGATCCTA CAGG-3′, strain Jajeri, nt 1224 to 1243) were used. The VP6 primers used in the RT-PCR were employed for VP6 gene sequencing (15).

DNA and protein sequence analysis. The chromatogram sequencing files were inspected using Chromas 2.23 (Technelysium, Queensland, Australia), and contigs were prepared using SeqMan II (DNASTAR, Madison, WI). Nucleotide and amino acid sequence similarity searches were performed using the National Center for Biotechnology Information (NCBI; National Institutes of Health, Bethesda, MD) BLAST (basic local alignment search tool) server on the GenBank database, release 145.0 (2). Multiple sequence alignments were calculated using CLUSTALX 1.81 (38). Sequences were manually edited in the GeneDoc, version 2.6.002, alignment editor.

Phylogenetic analysis. Phylogenetic and molecular evolutionary analyses were conducted using the MEGA version 2.1 software package (24). Genetic distances were calculated using the Kimura two-parameter model. The dendrograms were constructed using the neighbor-joining method.

Nucleotide sequence accession numbers. The nucleotide sequences reported in this paper were submitted to GenBank using National Center for Biotechnology Information (NCBI; Bethesda, MD) Sequin, version 5.00, under accession numbers AY754824 to AY754827.

RESULTS

Detection of group C rotaviruses. A total of 611 diarrheal stool specimens which were negative for group A rotaviruses were investigated for the presence of group C rotaviruses by PAGE and RT-PCR. Group C rotaviruses were detected in 14 samples (2.3% of the subset tested and 1.5% of the overall study) using one-step RT-PCR followed by a second PCR. PAGE could detect only one group C rotavirus strain with the characteristic 4-3-2-2 RNA migration pattern (Fig. 1).

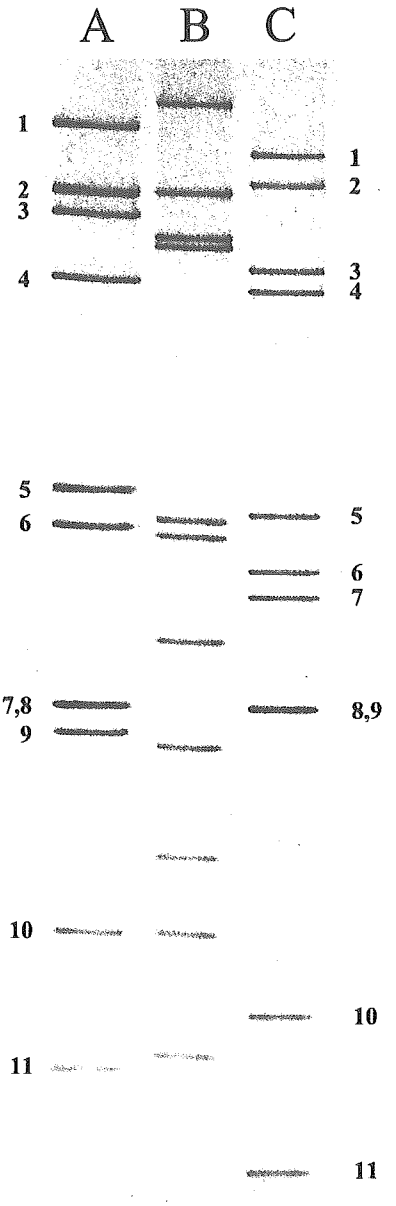

FIG. 1. Gel electrophoresis showing the characteristic genomic double-stranded RNA electrophoresis patterns of group A (lane A), group B (lane B), and group C (DhakaC13) (lane C) rotaviruses. The viral RNAs were analyzed by electrophoresis in a 10% polyacrylamide gel and visualized by staining with silver nitrate.

Clinical features of the group C rotavirus-infected patients. Clinical data of the 14 patients infected with group C rotaviruses are listed in Table 1. We found that eight group C rotavirus-infected patients (57.1%) had a variety of bacterial coinfections: six with *Vibrio cholerae* and two with *Shigella flexneri*. As the number of cases without coinfection was low ($n = 6$), it was difficult to determine whether the patient's clinical features were related to group C rotavirus and/or to the other pathogens.

Sequence analysis of the VP6 gene. The partial VP6 sequences (nt 1020 to 1329, corresponding to the VP6 gene of

TABLE 1. Clinical features of the patients infected with group C rotaviruses

Patient no.	Age (yr)	Sex	Abdominal pain	Vomiting	No. of stools per day	Duration (days) of diarrhea	Fever	Dehydration	Treatment[a]	Other pathogen
2339150	19.0	F	No	Yes	6–10 times	<1	No	Severe	IV to ORS	No
2344600	1.3	M	No	Yes	3–5 times	1–3	No	None	IV only	*S. flexneri*
2351250	35.0	M	Yes	Yes	16–20 times	<1	No	Severe	IV to ORS	No
2355500	26.0	M	Yes	Yes	6–10 times	<1	No	Moderate	IV to ORS	*V. cholerae* O1
2356950	1.0	F	No	Yes	6–10 times	1–3	No	Moderate	ORS only	No
2357500	2.0	M	No	Yes	11–15 times	1–3	No	Moderate	ORS only	*V. cholerae* O1
2357650	22.0	F	Yes	Yes	3–5 times	<1	No	Severe	IV to ORS	*V. cholerae* O1
2357700	2.0	M	Yes	Yes	6–10 times	1–3	No	Moderate	ORS only	No
2360450	4.0	M	No	Yes	6–10 times	<1	No	Severe	IV to ORS	*V. cholerae* O1
2360550	20.0	F	Yes	Yes	11–15 times	<1	No	Severe	IV to ORS	*V. cholerae* O1
2373100	0.8	M	No	Yes	3–5 times	4–6	Yes	None	ORS only	No
2373150	3.0	F	Yes	Yes	21+ times	<1	No	Severe	IV to ORS	*V. cholerae* O1
2374350	18.0	F	No	Yes	11–15 times	1–3	No	Severe	IV to ORS	No
2374700	3.0	M	Yes	No	6–10 times	1–3	No	None	ORS only	*S. flexneri*

[a] IV, intravenous fluid; ORS, oral rehydration solution.

the Jajeri strain) were determined for four group C rotavirus strains (DhakaC2, DhakaC4, DhakaC12, and DhakaC13) from the stool specimens with the most starting materials. They were almost identical to each other (99.3% nucleotide and 100% amino acid identities). Strain DhakaC13 was chosen as a representative of Bangladeshi group C rotaviruses. Sequence comparison revealed that the DhakaC13 strain had the greatest identity with the Jajeri strain, isolated in Nigeria, and with strain 208, isolated in China (98% nucleotide and 100% amino acid identities for both strains) (Table 2). Animal strains exhibited much less nucleotide and amino acid similarities with our DhakaC13 strain (82 to 84% nucleotide and 90 to 95% amino acid identities). A phylogenetic tree (Fig. 2) was constructed which included the partial nucleotide sequences of the published strains and the Bangladeshi strains (DhakaC2 and DhakaC13). Bangladeshi strains belonged to the human cluster, which was again distantly related to the animal clusters. A bovine strain (WD534tc) that has been suggested to be of porcine origin was found to belong to the porcine cluster as expected.

Sequence analysis of the VP4 gene. The partial VP4 gene sequence (nt 21 to 682) was determined for DhakaC13 and was compared with those of group C rotavirus strains available in the GenBank database (Table 3). The VP4 gene of DhakaC13 was closely related to the Nigerian Jajeri strain (98% identity at nucleotide and amino acid levels). Similarities with other human group C rotaviruses were also very high (96 to 97% at nucleotide levels and 94 to 96% at amino acid levels), whereas similarities with porcine and bovine group C rotaviruses were low (65 to 70% at the nucleotide level and 63 to 65% at the amino acid level). The phylogenetic tree revealed that three clusters were comprised of different host-specific strains (Fig. 3). DhakaC13 belonged to the human branch and was closely related to the Jajeri and Moduganari strains isolated from Nigeria. All human strains were distantly related to bovine and porcine clusters.

Sequence analysis of the VP7 gene. The complete coding nucleotide sequence (nt 49 to 1054) and deduced amino acid sequence of the VP7 gene of the DhakaC13 strain was determined and compared with VP7 gene sequences of other group C rotavirus strains available in the GenBank database. Table 4 shows the similarity of the published group C rotavirus strains with the DhakaC13 strain. Sequence comparison indicated that the VP7 sequence of the DhakaC13 strain was also most closely related to the Jajeri strain (97% identity at nucleotide and 99% identity at amino acid level). The VP7 sequences of all human rotavirus C strains were 95 to 99% identical at the nucleotide level and 96 to 99% at the amino acid level. The strains isolated from animals exhibited much less similarity to our DhakaC13 strain (73 to 82% nucleotide and 71 to 87%

TABLE 2. Nucleotide and amino acid sequence similarity between DhakaC13 and other group C rotavirus strains based on partial VP6 sequences[a]

Strain	Origin	Country	Accession no.	Identity (%) with DhakaC13	
				Nucleotide (nt 1020–1329)	Amino acid (aa 334–395)
Jajeri	Human	Nigeria	AF325805	98	100
208	Human	China	AB008672	98	100
Bristol	Human	U.K.	X59843	97	100
Moduganari	Human	Nigeria	AF325806	96	100
Belem	Human	Brazil	M94155	96	100
Preston	Human	U.K.	M94156	96	100
Cowden	Porcine	U.S.	M94157	84	95
Yamagata	Bovine	Japan	AB108680	83	93
Bos taurus	Bovine	U.S.	M88768	83	93
WD534tc	Bovine	U.S.	AF162434	82	90

[a] U.K., United Kingdom; U.S., United States; aa, amino acid.

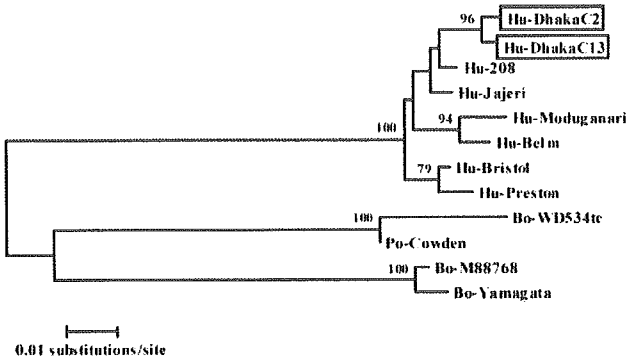

FIG. 2. Neighbor-joining phylogenetic tree based on partial nucleotide sequences (nt 1020 to 1329) of the VP6 genes for DhakaC13 and other established group C rotavirus strains. Bo, bovine; Hu, human; Po, porcine. The numbers adjacent to the nodes represent the percentage of bootstrap support (of 1,000 replicates) for the clusters to the right of the node. Bootstrap values lower than 75% are not shown.

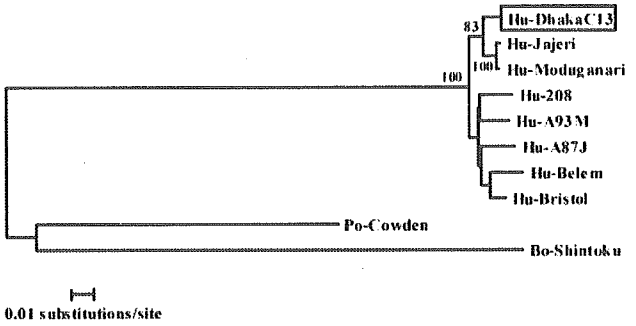

FIG. 3. Neighbor-joining phylogenetic tree based on the nucleotide sequences (nt 21 to 682) of partial VP8* fragments of the VP4 genes for DhakaC13 and other established group C rotavirus strains. Bo, bovine; Hu, human; Po, porcine. The numbers adjacent to the nodes represent the percentage of bootstrap support (of 1,000 replicates) for the clusters to the right of the node. Bootstrap values lower than 75% are not shown.

amino acid identities). Three conserved sites (amino acid positions 67 to 69, 152 to 154, and 225 to 227) that are potential N-glycosylation sites (Asn-X-Ser/Thr) were found in the VP7 deduced amino acid sequence of the DhakaC13 strain. A more detailed phylogenetic analysis that included all VP7 gene sequences of group C rotaviruses (Fig. 4) confirmed that our DhakaC13 strain belonged to the human group C rotavirus strains which clustered in a monophyletic branch, distantly related to the animal branches.

DISCUSSION

The present study is the first report of group C rotaviruses in Bangladesh. The low rate of detection suggests that group C rotavirus is an uncommon cause of gastroenteritis in hospitalized patients in Bangladesh. Moreover, the frequent association of group C rotavirus with other pathogens casts doubt on the pathogenic role of group C rotaviruses in these patients. Coinfections with pathogenic enteric bacteria were frequently observed in group C rotavirus-infected patients (57.1%) compared to the patients infected by group A rotaviruses (6.9%, n = 345; data not shown) during the same period.

The importance of group C rotaviruses in humans has been considered insignificant due to their sporadic nature, but the distribution of group C rotaviruses has recently been shown to be more common than previously believed according to a number of seroepidemiological surveys (9, 23, 25, 27, 30, 35, 36, 43). The true burden of group C rotaviruses might be underestimated due to difficulty in detecting them. In our study, PAGE was seen to be relatively insensitive. We could detect only one out of 14 PCR-confirmed group C rotavirus-positive stool specimens by this method. Likewise, pooling of the samples for RT-PCR resulted in a 1:10 dilution of our samples. For this reason, it is possible that we failed to detect some of the positive group C rotaviruses in the diluted specimens. Therefore, it is required that a less expensive enzyme immunoassay method be developed to detect and differentiate group C rotavirus G serotypes from a large-scale epidemiological study.

A formal classification system for group C rotaviruses has not yet been established, although at least four G types have been proposed by many investigators using sequence analysis of different human and animal group C rotavirus strains. For group A rotaviruses, it was observed that strains having more than 89% amino-acid-identical VP7 sequences belonged to the same G serotype (14). We studied the similarities between 45 complete VP7 amino acid sequences of all group C rotavirus strains available in GenBank (Table 5). The lineages were confirmed by the VP7 phylogenetic tree (Fig. 4). We found

TABLE 3. Nucleotide and amino acid sequence similarity between DhakaC13 and other group C rotavirus strains based on partial VP4 sequences[a]

Strain	Origin	Country	Accession no.	Identity (%) with DhakaC13	
				Nucleotide (nt 21–682)	Amino acid (aa 1–220)
Jajeri	Human	Nigeria	AF323981	98	98
Moduganari	Human	Nigeria	AF323980	98	98
208	Human	China	AB008670	97	96
A93M	Human	Australia	AY395070	96	94
A87J	Human	Australia	AY395069	96	96
Belem	Human	Brazil	X79441	96	96
Bristol	Human	U.K.	X79442	96	95
Cowden	Porcine	U.S.	M74218	70	65
Shintoku	Bovine	Japan	U26551	65	63

[a] U.K., United Kingdom; U.S., United States; aa, amino acids.

TABLE 4. Nucleotide and amino acid sequence similarity between DhakaC13 and other group C rotavirus strains based on partial VP7 sequences[a]

Strain	Origin	Country	Accession no.	Identity (%) with DhakaC13	
				Nucleotide (nt 49–1047)	Amino acid (aa 1–332)
Jajeri	Human	Nigeria	AF323982	97	99
Moduganari	Human	Nigeria	AF323979	97	98
Ad957	Human	U.S.	U20993	96	98
Santiago	Human	Argentina	U20996	96	98
Bristol	Human	U.K.	X77257	96	98
Belem	Human	Brazil	X77256	96	97
Uppsala/1004	Human	Sweden	AF225560	95	98
208	Human	China	AB008971	95	97
Solano	Human	Argentina	AF120478	95	96
I57	Human	Japan	AB086964	94	96
Cowden	Porcine	U.S.	M61101	83	87
WH	Porcine	U.S.	U31749	82	84
HF	Porcine	U.S.	U31748	75	71
Shintoku	Bovine	Japan	U31750	74	73

[a] U.K., United Kingdom; U.S., United States; aa, amino acids.

that the group C rotavirus strains could be clustered into four different groups if we consider 89% amino acid identity as a cutoff for grouping them. The porcine strain HF isolated in the United States and the bovine Shintoku strain isolated in Japan belonged to lineage 1 and lineage 2, respectively. The other two porcine strains, WH and Cowden, comprised a third lineage (lineage 3). All human strains clustered in a monophyletic branch (lineage 4).

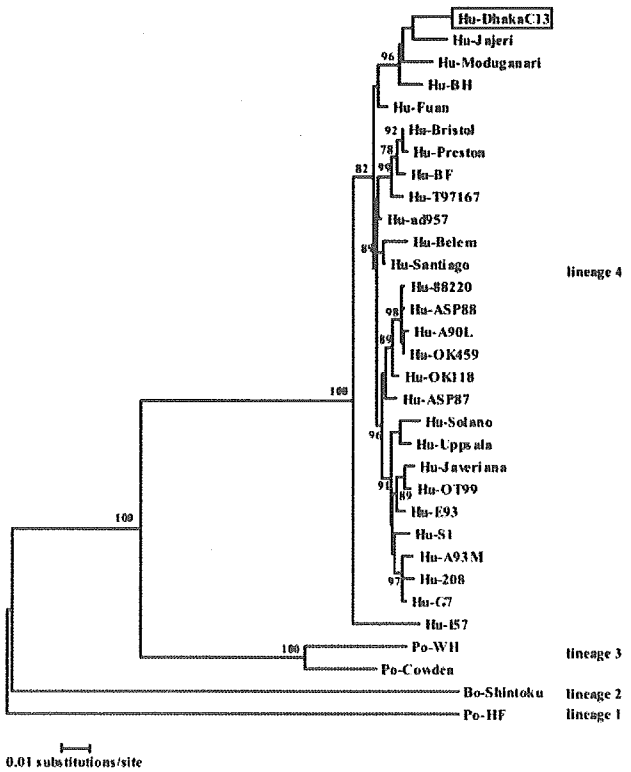

FIG. 4. Neighbor-joining phylogenetic tree based on nucleotide sequences (nt 49 to 1054) of the encoding regions of the VP7 gene for DhakaC13 and other established group C rotavirus. Bo, bovine; Hu, human; Po, porcine. The numbers adjacent to the nodes represent the percentage of bootstrap support (of 1,000 replicates) for the clusters to the right of the node. Bootstrap values lower than 75% are not shown.

Three P types were proposed by Jiang et al. (20) for group C rotavirus strains, which can be supported by the phylogenetic tree described in this paper (Fig. 2). However, since only eight VP4 gene sequences of human group C rotaviruses are available in GenBank, more sequences would be needed to better describe the P types of the group C rotavirus strains. We found that all human group C rotavirus strains clustered together in the same branch of the VP4 tree, which indicated one common ancestor of these strains.

Sequence analyses of the VP4, VP6, and VP7 genes of group C rotavirus strains revealed that the gene sequences are conserved and host restricted. These findings are supported by other group C rotavirus evolutionary studies (16, 21, 39). Further studies on the gene segments other than the VP4, VP6, and VP7 genes will be necessary to confirm whether the diversity of group C rotaviruses is really very low compared to group A rotaviruses.

Because this study is a hospital-based study, it is difficult to extrapolate our data to community rates of group C rotavirus infection, because only patients with significant dehydration were admitted. Moreover, older patients who are more frequently infected by group C rotaviruses usually do not go to hospitals unless the disease becomes extremely severe. Therefore, a community-based study would be required to investi-

TABLE 5. Amino acid sequence similarity matrix of VP7 proteins of group C rotavirus strains of four different lineages derived from the VP7 phylogenetic tree

VP7 lineage	% Similarity for lineage:			
	1	2	3	4
1	100			
2	72	100		
3	69–70	74	96	
4	70–71	72	84–87	96–100

[a] Lineage 1, porcine HF strain; lineage 2, bovine sintoku strain; lineage 3, porcine cowden and WH strains; lineage 4, human group C rotavirus strains available in GenBank.

gate the true prevalence and burden of disease of group C rotaviruses. At the same time, it will be necessary to develop more sensitive and easy-to-use diagnostic methods specific for human group C rotaviruses for large-scale epidemiological studies.

ACKNOWLEDGMENTS

This research study was funded by the ICDDR,B Centre for Health and Population Research and Flemish Fonds voor Wetenschappelijk, grant number G.0288.01.

REFERENCES

1. **Adah, M. I., A. Wade, M. Oseto, M. Kuzuya, and K. Taniguchi.** 2002. Detection of human group C rotaviruses in Nigeria and sequence analysis of their genes encoding VP4, VP6, and VP7 proteins. J. Med. Virol. **66:**269–275.
2. **Altschul, S., F. W. Gish, W. Miller, E. W. Myers, and D. J. Lipman.** 1990. Basic local alignment search tool. J. Mol. Biol. **215:**403–410.
3. **Bridger, J. C., I. N. Clarke, and M. A. McCrae.** 1982. Characterization of an antigenically distinct porcine rotavirus. Infect. Immun. **35:**1058–1062.
4. **Bridger, J. C., S. Pedley, and M. A. McCrae.** 1986. Group C rotaviruses in humans. J. Clin. Microbiol. **23:**760–763.
5. **Brown, D. W. G., M. M. Mathan, M. Mathew, R. Martin, G. M. Beards, and V. I. Mathan.** 1988. Rotavirus epidemiology in Vellore, South India: group, subgroup, serotype, and electrophreotype. J. Clin. Microbiol. **26:**2410–2414.
6. **Castello, A. A., M. H. Arguelles, G. A. Villegas, A. Olthoff, and G. Glikmann.** 2002. Incidence and prevalence of human group C rotavirus infections in Argentina. J. Med. Virol. **67:**106–112.
7. **Castello, A. A., M. H. Arguelles, G. A. Villegas, N. Lopez, D. P. Ghiringhelli, L. Semorile, and G. Glikmann.** 2000. Characterization of human group C rotavirus in Argentina. J. Med. Virol. **62:**199–207.
8. **Chen, H. J., B. S. Chen, S. F. Wang, and M. H. Lai.** 1991. Rotavirus gastroenteritis in children: a clinical study of 125 patients in Hsin-Tien area. Zhonghua Min Guo Xiao Er Ke Yi Xue Hui Za Zhi **32:**73–78.
9. **Cunliffe, N. A., W. Dove, B. Jiang, B. D. Thinwda Cert, R. L. Broadhead, M. E. Molyneux, and C. A. Hart.** 2001. Detection of group C rotavirus in children with acute gastroenteritis in Blantyre, Malawi. Pediatr. Infect. Dis. J. **20:**1088–1090.
10. **Espejo, R. T., and F. Puerto.** 1984. Shifts in the electrophoretic pattern on the RNA genome of rotaviruses under different electrophoretic conditions. J. Virol. Methods **8:**293–299.
11. **Estes, M. K.** 2001. Rotaviruses and their replication, p. 1747–1786. *In* D. M. Knipe, P. M. Howley, D. E. Griffin, R. A. Lamb, M. A. Martin, B. Roizman, and S. E. Straus (ed.), Fields virology, 4th ed., vol. 2. Lippincott Williams & Wilkins, Philadelphia, Pa.
12. **Fielding, P. A., P. R. Lambden, E. O. Caul, and I. N. Clarke.** 1994. Molecular characterization of the outer capsid spike protein (VP4) gene from human group C rotavirus. Virology **204:**442–446.
13. **Fujii, R., M. Kuzuya, M. Hamano, H. Ogura, M. Yamada, and T. Mori.** 2000. Neutralization assay for human group C rotaviruses using a reverse hemagglutination test for endpoint determination. J. Clin. Microbiol. **38:**50–54.
14. **Gentsch, J. R., P. A. Woods, M. Ramachandran, B. K. Das, J. P. Leite, A. Alfieri, R. Kumar, M. K. Bhan, and R. I. Glass.** 1996. Review of G and P typing results from a global collection of rotavirus strains: implications for vaccine development. J. Infect. Dis. **174:**S30–S36.
15. **Gouvea, V., J. R. Allen, R. I. Glass, Z. Y. Fang, M. Bremont, J. Cohen, M. A. McCrae, L. J. Saif, P. Sinarachatanant, and E. O. Caul.** 1991. Detection of group B and C rotaviruses by polymerase chain reaction. J. Clin. Microbiol. **29:**519–523.
16. **Grice, A. S., P. R. Lambden, E. O. Caul, and I. N. Clarke.** 1994. Sequence conservation of the major outer capsid glycoprotein of human group C rotaviruses. J. Med. Virol. **44:**166–171.
17. **Herring, A. J., N. F. Inglis, C. K. Ojeh, D. R. Snodgrass, and J. D. Menzies.** 1982. Rapid diagnosis of rotavirus infection by direct detection of viral nucleic acid in silver-stained polyacrylamide gels. J. Clin. Microbiol. **16:**473–477.
18. **James, V. L. A., P. R. Lambden, E. O. Caul, and I. N. Clarke.** 1998. Enzyme-linked immunosorbent assay based on recombinant human group C rotavirus inner capsid protein (VP6) to detect human group C rotaviruses in fecal samples. J. Clin. Microbiol. **36:**3178–3181.
19. **James, V. L., P. R. Lambden, E. O. Caul, S. J. Cooke, and I. N. Clarke.** 1997. Seroepidemiology of human group C rotavirus in the UK. J. Med. Virol. **52:**86–91.
20. **Jiang, B., J. R. Gentsch, H. Tsunemitsu, L. J. Saif, and R. I. Glass.** 1999. Sequence analysis of the gene encoding VP4 of a bovine group C rotavirus: molecular evidence for a new P genotype. Virus Genes **19:**85–88.
21. **Jiang, B., H. Tsunemitsu, P. H. Dennehy, I. Oishi, D. Brown, R. D. Schnagl, M. Oseto, Z. Y. Fang, L. F. Avendano, L. J. Saif, and R. I. Glass.** 1996. Sequence conservation and expression of the gene encoding the outer capsid glycoprotein among human group C rotaviruses of global distribution. Arch. Virol. **141:**381–390.
22. **Jiang, B., P. H. Dennehy, S. Spangenberger, J. Gentsch, and R. I. Glass.** 1995. First detection of group C rotaviruses in faecal specimens of children with diarrhoea in the United States. J. Infect. Dis. **172:**45–50.
23. **Kapikian, A. Z., Y. Hoshino, and R. M. Chanock.** 2001. Rotaviruses, p. 1787–1833. *In* D. M. Knipe, P. M. Howley, D. E. Griffin, R. A. Lamb, M. A. Martin, B. Roizman, and S. E. Straus (ed.), 4th ed., vol. 2. Lippincott Williams & Wilkins, Philadelphia, Pa.
24. **Kumar, S., K. Tamura, I. B. Jakobsen, and M. Nei.** 2001. MEGA2: molecular evolutionary genetics analysis software. Bioinformatics **17:**1244–1245.
25. **Kuzuya, M., R. Fujii, M. Hamano, M. Yamada, K. Shinozaki, A. Sasagawa, S. Hasegawa, H. Kawamoto, K. Matsumoto, A. Kawamoto, A. Itagaki, S. Funatsumaru, and S. Urasawa.** 1998. Survey of human group C rotaviruses in Japan during the winter of 1992 to 1993. J. Clin. Microbiol. **36:**6–10.
26. **Nagesha, H. S., C. P. Hum, J. C. Bridger, and I. H. Holmes.** 1988. Atypical rotaviruses in Australian pigs. Arch. Virol. **102:**91–98.
27. **Nilsson, M., B. Svenungsson, K. O. Hedlund, I. Uhnoo, A. Lagergren, T. Akre, and L. Svensson.** 2000. Incidence and genetic diversity of group C rotavirus among adults. J. Infect. Dis. **182:**678–684.
28. **Oseto, M., Y. Yamashita, M. Hattori, M. Mori, H. Inoue, Y. Ishimaru, and S. Matsuno.** 1994. Serial propagation of human group C rotavirus in a continuous cell line (CaCo-2). J. Clin. Exp. Med. **168:**177–178. (In Japanese.)
29. **Rasool, N. B. G., M. Hamzah, M. Jegathesan, Y. H. Wong, Y. Qian, and K. Y. Green.** 1994. Identification of a human group C rotavirus in Malaysia. J. Med. Virol. **43:**209–211.
30. **Riepenhoff-Talty, M., K. Morse, C. H. Wang, C. Shapiro, J. Roberts, M. Welter, M. Allen, M. J. Evans, and T. D. Flanagan.** 1997. Epidemiology of group C rotavirus infection in western New York women of childbearing age. J. Clin. Microbiol. **35:**486–488.
31. **Rodger, S. M., R. F. Bishop, and I. H. Holmes.** 1982. Detection of a rotavirus-like agent associated with diarrhea in an infant. J. Clin. Microbiol. **16:**724–726.
32. **Saif, L. J.** 1990. Nongroup A rotaviruses, p. 73–95. *In* L. J. Saif and K. W. Theil (ed.), Viral diarrhea of man and animals. CRC Press, Boca Raton, Fla.
33. **Saif, L. J., and B. Jiang.** 1994. Non-group A rotaviruses of humans and animals. Curr. Top. Microbiol. Immunol. **85:**339–371.
34. **Saif, L. J., E. H. Bohl, K. W. Theil, R. F. Cross, and J. A. House.** 1980. Rotavirus-like, calicivirus-like, and 23-nm virus-like particles associated with diarrhea in young pigs. J. Clin. Microbiol. **12:**105–111.
35. **Sanchez-Fauquier, A., E. Roman, J. Colomina, I. Wilhelmi, R. I. Glass, and B. Jiang.** 2003. First detection of group C rotavirus in children with acute diarrhea in Spain. Arch. Virol. **148:**399–404.
36. **Steele, A. D., and V. L. James.** 1999. Seroepidemiology of human group C rotavirus in South Africa. J. Clin. Microbiol. **37:**4142–4144.
37. **Stoll, B. J., R. I. Glass, M. I. Huq, M. U. Khan, J. E. Holt, and H. Banu.** 1982. Surveillance of patients attending a diarrhoeal disease hospital in Bangladesh. Br. Med. J. **285:**1185–1188.
38. **Thompson, J. D., D. G. Higgins, and T. J. Gibson.** 1994. CLUSTAL W: improving the sensitivity of progressive multiple sequence alignment through sequence weighting, position-specific gap penalties and weight matrix choice. Nucleic Acids Res. **22:**4673–4680.
39. **Tsunemitsu, H., B. Jiang, Y. Yamashita, M. Oseto, H. Ushijima, and L. Saif.** 1992. Evidence of serologic diversity within group C rotaviruses. J. Clin. Microbiol. **30:**3009–3012.
40. **Tsunemitsu, H., B. Jiang, and L. J. Saif.** 1992. Detection of group C rotavirus antigens and antibodies in animals and humans by enzyme-linked immunosorbent assays. J. Clin. Microbiol. **30:**21–29.
41. **Ushijima, H., H. Honma, A. Mukyama, T. Shinozaki, Y. Fujita, M. Kobayashi, M. Ohseto, S. Morikawa, and T. Kitamura.** 1989. Detection of group C rotaviruses in Tokyo. J. Med. Virol. **27:**299–303.
42. **von Bonsdorff, C. H., and L. Svensson.** 1988. Human serogroup C rotavirus in Finland. Scand. J. Infect. Dis. **20:**475–478.
43. **Wu, H., K. Taniguchi, T. Urasawa, and S. Urasawa.** 1998. Serological and genomic characterization of human rotaviruses detected in China. J. Med. Virol. **55:**168–176.

JOURNAL OF VIROLOGY, Feb. 2006, p. 1513–1523 Vol. 80, No. 3
0022-538X/06/$08.00+0 doi:10.1128/JVI.80.3.1513–1523.2006

High-Resolution Molecular and Antigen Structure of the VP8* Core of a Sialic Acid-Independent Human Rotavirus Strain†

Nilah Monnier,[1,2] Kyoko Higo-Moriguchi,[3] Zhen-Yu J. Sun,[4] B. V. Venkataram Prasad,[5] Koki Taniguchi,[3] and Philip R. Dormitzer[2,6]*

Harvard College, Cambridge, Massachusetts 02138[1]; Laboratory of Molecular Medicine, Children's Hospital, Boston, Massachusetts 02115[2]; Department of Virology and Parasitology, Fujita Health University School of Medicine, Toyoake, Aichi 470-1192, Japan[3]; Department of Biological Chemistry and Molecular Pharmacology, Harvard Medical School, Boston, Massachusetts 02115[4]; Verna and Marrs McLean Department of Biochemistry and Molecular Biology, Baylor College of Medicine, One Baylor Plaza, Houston, Texas 77030[5]; and Department of Pediatrics, Harvard Medical School, Boston, Massachusetts 02115[6]

Received 22 July 2005/Accepted 25 October 2005

The most intensively studied rotavirus strains initially attach to cells when the "heads" of their protruding spikes bind cell surface sialic acid. Rotavirus strains that cause disease in humans do not bind this ligand. The structure of the sialic acid binding head (the VP8* core) from the simian rotavirus strain RRV has been reported, and neutralization epitopes have been mapped onto its surface. We report here a 1.6-Å resolution crystal structure of the equivalent domain from the sialic acid-independent rotavirus strain DS-1, which causes gastroenteritis in humans. Although the RRV and DS-1 VP8* cores differ functionally, they share the same galectin-like fold. Differences between the RRV and DS-1 VP8* cores in the region that corresponds to the RRV sialic acid binding site make it unlikely that DS-1 VP8* binds an alternative carbohydrate ligand in this location. In the crystals, a surface cleft on each DS-1 VP8* core binds N-terminal residues from a neighboring molecule. This cleft may function as a ligand binding site during rotavirus replication. We also report an escape mutant analysis, which allows the mapping of heterotypic neutralizing epitopes recognized by human monoclonal antibodies onto the surface of the VP8* core. The distribution of escape mutations on the DS-1 VP8* core indicates that neutralizing antibodies that recognize VP8* of human rotavirus strains may bind a conformation of the spike that differs from those observed to date.

Rotavirus is the most important cause of severely dehydrating childhood gastroenteritis worldwide (37). To prime the nonenveloped virion for host membrane penetration, intestinal trypsin cleaves the rotavirus spike protein, VP4, into two fragments, VP8* and VP5* (15). In some strains, VP8* mediates initial attachment to target cells by binding cell surface sialic acid (SA) (6, 16). In electron cryomicroscopy image reconstructions of trypsin-primed, SA-dependent virions, the protruding part of the spikes has approximate twofold symmetry (Fig. 1). It is tipped by paired heads, separated by a small gap (41, 44). The heads are formed by a globular domain of VP8* (14). We refer to this globular domain as the "VP8* core," because it remains intact following limit protease digestion of recombinant VP4 (12). VP5* forms more virion-proximal parts of the spikes (Fig. 1) and has a hydrophobic apex (13), which has been implicated as a potential membrane penetration region (32). VP8* masks the hydrophobic apex of VP5* on primed spikes (13). During cell entry, VP8* probably separates from VP5*, exposing the hydrophobic apex and allowing a fold-back rearrangement of VP5*. Some antibodies that bind VP8* appear to neutralize virus by triggering uncoating—the shedding of VP4 or its fragments and the coat protein VP7 (45). This mechanism of neutralization suggests that conformational changes involving VP8* could trigger subsequent entry events, such as VP5* rearrangement and outer-layer disassembly. VP8* may also function intracellularly, binding intracellular tumor necrosis factor receptor-associated factors to activate cellular signaling pathways (28).

Although SA was the first rotavirus receptor identified (2), most rotavirus strains do not, in fact, bind this receptor during entry (6). None of the strains that are known to be virulent in humans bind SA (6). Differences between SA-dependent and SA-independent strains extend beyond the ability or inability of their spike proteins to bind SA: SA-independent strains are generally more fastidious in cell culture than SA-dependent strains (40, 42), and although SA-independent strains infect polarized epithelial cells from either the apical or basolateral membrane, SA-dependent strains enter only at the apical surface (4).

The VP8* core is an important target of neutralizing antibodies against rotavirus (reviewed in reference 14). Some neutralizing monoclonal antibodies (MAbs) that recognize this domain on SA-dependent strains protect mouse pups from rotavirus diarrhea when present in the gut lumen (33). The VP8* core is the major determinant of P serotype (which correlates reasonably well with P genotype) for both SA-dependent and SA-independent strains (22). Therefore, this domain contains key neutralization determinants for both functional variants. While most VP4-specific MAbs that neutralize SA-dependent rotavirus virions map to the VP8* fragment, most VP4-specific MAbs that neutralize SA-independent virions map to the VP5* fragment (reviewed in reference 25). It is not known whether this difference reflects biological differences between SA-dependent and SA-

* Corresponding author. Mailing address: Laboratory of Molecular Medicine, Enders 673, Children's Hospital, Boston, MA 02115. Phone: (617) 355-3026. Fax: (617) 730-1967. E-mail: dormitze@crystal.harvard.edu.

† Supplemental material for this article may be found at http://jvi.asm.org.

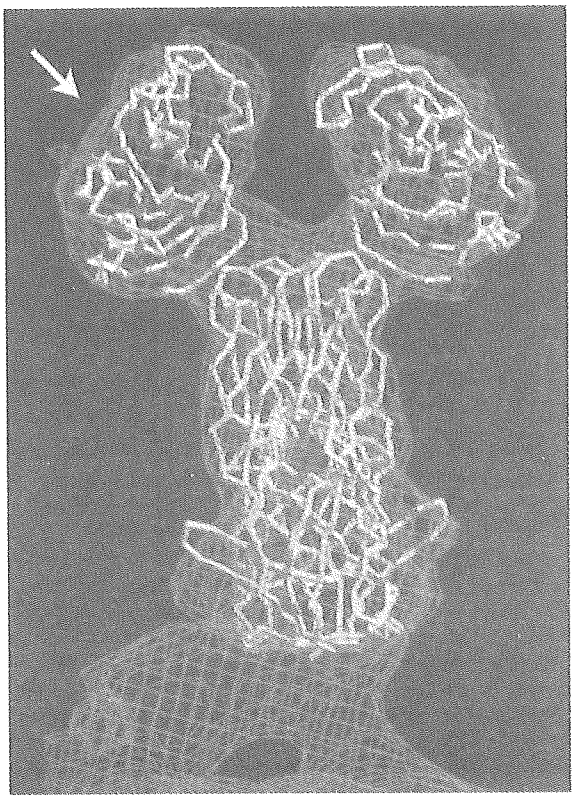

FIG. 1. The rotavirus VP4 spike. The Cα traces of the VP8* core (white) and a globular domain of VP5* (yellow) from RRV are fitted to the molecular envelope of the VP4 spike in an approximately 12-Å-resolution electron cryomicroscopy image reconstruction of a primed SA11-4F rotavirus virion. The arrow indicates the perspective of the depictions in Fig. 3 and 4B.

independent strains or the use of different strategies to screen hybridomas.

Although understanding the structure and function of SA-independent strains is particularly important for understanding and preventing rotavirus gastroenteritis in humans, SA-independent strains are less studied than SA-dependent strains. X-ray crystal and nuclear magnetic resonance (NMR) solution structures of the VP8* core of an SA-dependent simian rotavirus strain (RRV) have been obtained (14), but neither electron cryomicroscopy-based image reconstructions nor high-resolution structures are available for any SA-independent strain. Therefore, the structural basis for the differences in VP8* function is not known. Here, we present the X-ray crystal structure of the VP8* core from rotavirus strain DS-1, an SA-independent P genotype 4 strain that causes gastroenteritis in humans. We also report neutralization escape mutations of VP8* selected by two human monoclonal antibodies derived from cDNA of B lymphocytes from naturally infected humans. Mapping neutralization escape mutations onto the DS-1 VP8* core structure suggests that VP8*-specific antibodies that neutralize SA-dependent and SA-independent rotavirus strains recognize different conformations of the spike protein.

MATERIALS AND METHODS

Subcloning of the DS-1 and KU VP8* cores. Genes encoding the VP8* cores of rotavirus strains DS-1 and KU were subcloned from recombinant baculoviruses that contain the full-length DS-1 and KU VP4 coding sequences (18). Primers to amplify the KU VP8* coding sequence were designed based on a previously banked KU VP4 sequence (GenBank accession code M21014). The sequence of the DS-1 VP8* core was determined from DNA amplified by PCR from the recombinant baculovirus using primers complementary to sequences in the BlueBac2 vector on either side of the VP4 coding sequence. The sequences encoding KU and DS-1 VP4 residues 60 to 223 (the VP8* cores) were isolated as PCR products with XhoI and NotI ends and with a potential trypsin cleavage site just N terminal to residue 60. Each fragment was subcloned into the multiple cloning site of a pGex 4T-1 vector (Amersham Biosciences) that had been digested with SalI and NotI.

Expression and purification of recombinant VP8* cores. The RRV, DS-1, and KU VP8* cores were expressed in *Escherichia coli* strain BL21 and purified as described previously (14). Overnight cultures were diluted 1:100 in LB containing 0.1 mg/ml ampicillin and incubated at 37°C. When the cultures reached an A_{600} of about 0.6, the temperature was reduced to 25°C. After 30 to 60 min of incubation at 25°C, isopropyl-β-D-thiogalactopyranoside (IPTG) was added to 1 mM. The cultures were then incubated for an additional 4 h at 25°C before being harvested. Pelleted bacteria were lysed by sonication. The lysates were clarified by centrifugation in a Ti45 rotor (Beckman) at 40,000 rpm for 2 h at 4°C. The clarified lysates were passed over a glutathione-Sepharose column (Amersham Biosciences), and the VP8* cores were cleaved from the bound glutathione *S*-transferase (GST) tags by incubation on the column with 5 μg/ml tosylsulfonyl phenylalanyl chloromethyl ketone-treated trypsin (Worthington Biochemical) in TNC (20 mM Tris, pH 8.0, 100 mM NaCl, 1 mM $CaCl_2$) for 2 h at room temperature. The trypsin was removed from the released VP8* by passage over a benzamidine-Sepharose column (Amersham Biosciences), and any residual tryptic activity was eliminated by the addition of 1 mM phenylmethylsulfonyl fluoride and 2.5 mM benzamidine. The VP8* cores were further purified by size exclusion chromatography on a Superdex 200 column (Amersham Biosciences) in TNE (20 mM Tris, pH 8.0, 100 mM NaCl, 1 mM EDTA) at 4°C using a fast-protein liquid chromatography system (Amersham Biosciences).

Crystallization. The DS-1 VP8* core crystallized in space group P1 with the following unit cell parameters: a = 42.42 Å, b = 84.12 Å, c = 90.77 Å, α = 90.03°, β = 90.02°, and γ = 75.54°. The crystals have a solvent content of 38.5%, and each asymmetric unit contains eight VP8* cores. Crystals formed within 1 week at 20°C in hanging drops, with a sample solution containing 5 to 10 mg/ml protein in TNE-0.02% sodium azide-0.1 mM benzamidine, mixed 1:1 with a well solution containing 20% polyethylene glycol 4000, 500 mM sodium chloride, 100 mM sodium citrate, pH 5.6, and 3% ethanol or ethylene glycol. Harvested crystals were soaked in a cryoprotectant solution containing 22% polyethylene glycol 4000, 550 mM sodium chloride, 100 mM sodium citrate, pH 5.6, 3% ethanol or ethylene glycol, 15% glycerol and then frozen by rapid immersion in liquid nitrogen.

X-ray diffraction data collection and processing. X-ray diffraction data were collected at 100 K and a wavelength of 0.916 Å using beam line F1 at the Cornell High Energy Synchrotron Source. Diffracted X rays were detected by an ADSC Quantum 4 charge-coupled device. Diffraction data were indexed, integrated, and scaled using HKL2000 (HKL Research, Inc.). (For scaling statistics, see Table 2.)

Structure determination and refinement. The DS-1 VP8* core structure was determined by molecular replacement, using an initial phasing model based on the previously determined structure of the SA-bound RRV VP8* core (14). Rotation and translation solutions were determined using CNS (3). The structure was refined by multiple cycles of simulated annealing, energy minimization, and individual B-factor refinement using CNS (3). The model was rebuilt in O (24) using simulated annealing omit maps calculated in CNS (3) to eliminate phasing bias from the molecular replacement model. The geometry of the structures was analyzed using PROCHECK (29). (For refinement statistics, see Table 2.)

NMR spectroscopy. Purified protein for NMR was prepared as described above, except that size exclusion chromatography was carried out in 20 mM sodium phosphate, pH 7.0–100 mM NaCl, and the resulting protein sample was dialyzed into 20 mM sodium phosphate, pH 7.0–10 mM NaCl. The assayed peptide was ^{15}N labeled on valine and had the sequence TVEPVS, corresponding to DS-1 VP4 residues 60 to 64 plus a C-terminal serine. To avoid competition between the peptide and residues of the authentic N-terminal leader of the unlabeled DS-1 VP8* core, residues 60 to 64 of the core were mutated to SGSGG using PCR. Samples were made 10% in D_2O for field locking. Spectra were obtained at 25°C using a 500-MHz Bruker spectrometer equipped with a cryoprobe. Two-dimensional ^{15}N-^{1}H heteronuclear single quantum coherence spectra showed no change in the chemical shifts of the ^{15}N valines of the peptide when 0.29 mM DS-1 VP8* core was mixed with 0.1 mM peptide. NMR data were processed using PROSA (20), and spectra were analyzed using XEASY (1).

Structural analysis and figure production. Structure alignments were calculated using LSQKAB in CCP4 (7). Amino acid variability was calculated by AMAS (30). To determine the accessibility of VP8* core surfaces for antibody binding on trypsin-primed virions, the DS-1 VP8* core structure was aligned with an RRV VP8* core structure that had been fitted to an approximately 12-Å electron cryomicroscopy-based envelope of trypsin-primed SA11-4F rotavirus particles, contoured at 0.5 σ, as previously described (13). The envelope and fitted crystal structure were probed with the crystal structure of an Fab of a human immunoglobulin G1(κ) in complex with Lewis Y nonoate methyl ester (Protein Data Bank accession code 1CLY) using O (23, 24). Residues that could be brought into contact with any portion of the antigen-combining site were scored as accessible. The figures were made using GRASP (34), MOLSCRIPT (27), Illustrator (Adobe Systems, Inc.), and Photoshop (Adobe Systems, Inc.).

Selection of neutralization escape mutants. Rotavirus strain KU (30 μl; 3.6×10^5 PFU) was pretreated with trypsin (10 μg/ml) and mixed with 70 μl of purified 1-2H (200 μg/ml) or 2-3E (50 μg/ml) Fab in Eagle's minimum essential medium (MEM). After 1 h of incubation at 37°C, the virus-antibody mixtures were inoculated onto MA104 cell monolayers in 1 ml of Eagle's MEM in roller tubes (15 mm by 15 cm). After adsorption for 1 h, the monolayers were washed with phosphate-buffered saline and then incubated in a rotator (RT-550; Taitec Inc.) with 1 ml of Eagle's MEM containing purified 1-2H (100 μg/ml) or 2-3E (25 μg/ml) antibody and trypsin (5 μg/ml). Cultures were harvested 7 days after infection. After three rounds of propagation in the presence of neutralizing antibody, the selected viruses were plaque purified on CV-1 cells.

Sequencing of rotavirus variants. Full-length cDNA encoding VP4 and VP7 was prepared by reverse transcription-PCR. Nucleotide sequences were determined directly from the PCR products using ABI Prism BigDye Terminator Cycle Sequencing Ready Reaction Kits (PE Biosystems) with an automated sequencer, the ABI Prism 310 Genetic Analyzer (PE Applied Biosystems). The VP4-encoding genes of the two selected viruses each differed from the parental gene by a single nucleotide substitution. The VP7-encoding genes contained no mutations.

Protein structure and nucleotide sequence accession numbers. The atomic coordinates and structure factor amplitudes for the DS-1 VP8* core have been deposited in the Protein Data Bank under accession code 2AEN. Nucleotide sequences have been deposited in GenBank with the following accession codes: DS-1 VP8* core, DQ141310; KU VP4 clone 1, AB222784; M-KU-1-2H, AB222785; M-KU-2-3E, AB222786.

RESULTS AND DISCUSSION

Expression, purification, and stability of rotavirus VP8* cores. The VP8* core is a compact domain that presents conformational neutralizing epitopes. Our previously reported data demonstrate that the RRV VP8* core (P genotype 3) can be expressed in *E. coli* as a soluble GST fusion protein (14). After glutathione affinity chromatography, the domain can be separated from its GST tag by trypsin cleavage and purified by size exclusion chromatography with high yield as a homogeneous, protease-resistant, and very soluble protein (14).

We tested whether the VP8* core of an SA-independent strain that causes gastroenteritis in humans has similarly favorable characteristics. When expressed and purified using the protocol developed for the RRV VP8* core, the DS-1 VP8* core (P genotype 4) was obtained in good yield as a homogeneous, protease-resistant, soluble, pure protein (Fig. 2A and Table 1). As assayed by size exclusion chromatography, sodium dodecyl sulfate-polyacrylamide gel electrophoresis (SDS-PAGE), matrix-assisted laser desorption ionization mass spectrometry, and N-terminal sequencing, the RRV and DS-1 VP8* cores remain intact, homogeneous, and soluble after storage at 4°C for approximately 2 years (Fig. 2A, Table 1, and data not shown).

This purification procedure is also effective at producing a homogeneous VP8* core from a P genotype 8, SA-independent rotavirus strain, KU (Fig. 2B and Table 1). Together, P genotypes 4 and 8 cause more than 90% of human cases of rotavirus gastroenteritis in temperate climates (11). Although the KU VP8* core is also very soluble, it is produced in relatively low yield and undergoes substantially more degradation and aggregation with storage than do the RRV and DS-1 VP8*

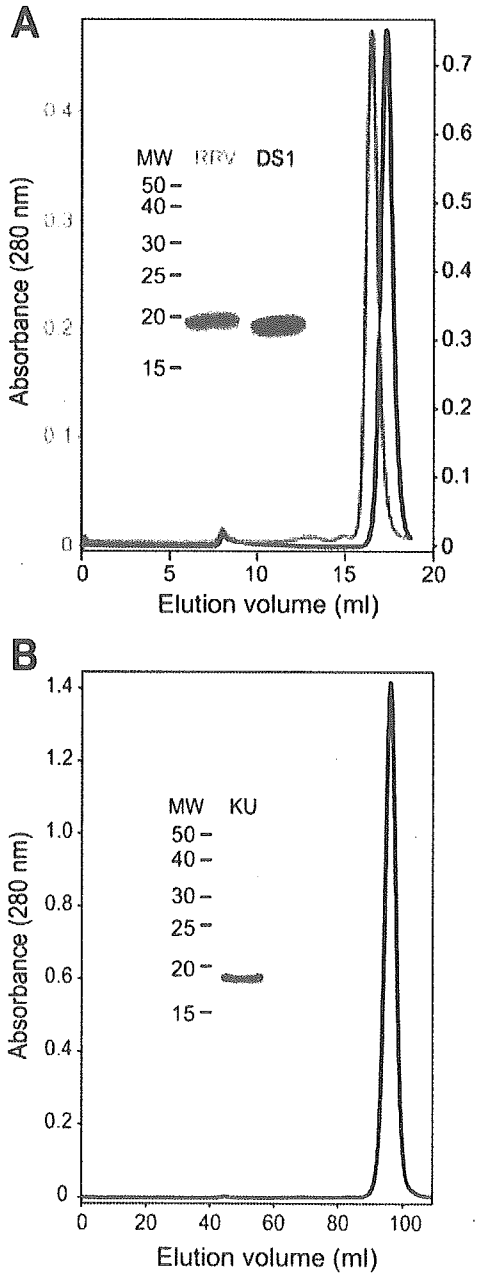

FIG. 2. Size exclusion chromatography and SDS-PAGE of purified VP8* cores. (A) Chromatograms of RRV (red) and DS-1 (blue) VP8* cores, which were separated on a Superdex 200 10/30 column at 4°C in TNE after storage for 2 years at 4°C in TNE with 0.02% sodium azide and 0.1 mM benzamidine. The inset image of a Coomassie blue-stained SDS-PAGE gel shows stored samples prior to chromatography. (B) Chromatogram of a freshly prepared sample of the KU VP8* core, which was separated on a Hi-Load Superdex 200 16/60 column at 4°C in TNE. The inset image of a Coomassie-blue stained SDS-PAGE gel shows protein from the pooled peak fractions. Apparent molecular masses that correspond to peak elution volumes are listed in Table 1.

TABLE 1. Biochemical characteristics of the RRV, DS-1, and KU VP8* cores

Characteristic	Value		
	RRV	DS-1	KU
No. of rotavirus VP4 residues in construct	60–224	60–223	60–223
Predicted MW	18570.6	18758.3	18882.4
MW fresh[a]	18592.8	18826.8	19104.4
MW after storage[a]	18568.2	18734.3	Multiple fragments
Length of storage (days)	798	718	767
Apparent mass (kDa)[b]	23.6 (after storage)	17.4 (after storage)	7.9 (fresh)[c]
Yield (mg/liter of bacterial culture)[d]	16	8.6	2.6
Solubility (mg/ml)	≥88	≥39.1	≥22.7

[a] Determined by matrix-assisted laser desorption ionization mass spectrometry.
[b] Based on elution volume by gel filtration chromatography (Fig. 2).
[c] This anomalously low apparent molecular mass probably results from affinity of the KU VP8* core for the chromatography medium.
[d] Yield refers to the final purified VP8* core.

cores (Fig. 2B, Table 1, and data not shown). Thus, the biochemical characteristics of the RRV and DS-1 VP8* cores make them promising potential immunogens for use in recombinant rotavirus vaccines. The less favorable characteristics of the KU VP8* core indicate that developing an antigenic cocktail of VP8* cores to completely cover the P types causing human disease will require screening of additional strains and possibly protein engineering.

Structural comparison of the DS-1 and RRV VP8* cores. Using the X-ray crystal structure of the RRV VP8* core as an initial phasing model for molecular replacement, we determined the X-ray crystal structure of the DS-1 VP8* core at 1.6-Å resolution (see Materials and Methods) (Table 2). The DS-1 VP8* core, like the RRV VP8* core, resembles the galectins, a family of animal lectins, in its fold. It is built around a central β-sandwich, with a β-hairpin (strands E and F) packed against a six-stranded β-sheet and a C-terminal α-helix packed against a five-stranded β-sheet (Fig. 3A). Each asymmetric unit contains eight molecules of the DS-1 VP8* core. There are no major conformational differences between the eight molecules, which can be superimposed on each other with an average root mean square deviation (RMSD) between Cα atoms of 0.26 Å (not shown).

Although the DS-1 and RRV VP8* cores have only 45% amino acid identity (for residues 65 to 224 of RRV and 65 to 223 of DS-1), they can be superimposed on each other with an RMSD of 1.04 Å for 159 equivalent Cα atoms (Fig. 3B). The broad surface that is formed by the EF β-hairpin, strands H and G of the six-stranded β-sheet, and strands J and K of the five-stranded β-sheet is furrowed by two clefts (Fig. 3A to D). Both clefts are wider in the DS-1 VP8* core than in the RRV VP8* core (Fig. 3B). In the DS-1 VP8* core, the architecture of the cleft corresponding to the RRV SA binding site, which lies between the five-stranded and six-stranded β-sheets, is extensively reworked (Fig. 3C to F). In the RRV VP8* core, the R101 side chain amide makes key contacts with SA. It projects from strand D to the floor of the binding site to form a positively charged surface patch and makes bidentate hydrogen bonds to the glycerol group of the bound carbohydrate (Fig. 3D and F). In the DS-1 VP8* core, phenylalanine replaces arginine at this site and has a very different structural role. F101 of DS-1 makes no contribution to the molecular surface (Fig. 3C); instead, its aromatic ring forms part of a hydrophobic core in the interface between the β-sheets (Fig. 3E). In the RRV VP8* core, the aromatic rings of Y155 and Y188 project out into solvent to form walls on either side of the SA binding pocket (Fig. 3D and F). In the DS-1 VP8* core, replacement of these residues by R154 and S187 removes these walls. In fact, the R154 side chain replaces the floor of the SA binding pocket with a low ridge, as it stretches across the gap between the six- and five-stranded β-sheets (Fig. 3C and E). Although the structural data do not exclude the possibility that an alternative carbohydrate ligand binds in place of SA in

TABLE 2. Crystallographic data collection and refinement statistics

Statistic	Value
Data collection	
Resolution limit (Å)	1.6
No. of unique reflections	153,466
Redundancy[a]	1.95 (1.72)
Completeness[a] (%)	96.8 (94.7)
I/σ[a]	17.2 (3.4)
R_{sym}[a,b] (%)	5.0 (37.6)
Refinement	
No. of polypeptide chains	8
No. of protein atoms	10,762
No. of water molecules	1,724
No. of glycerol molecules	6
No. of ethanol molecules	4
No. of amino acids with alternative conformations	43
Residues in allowed regions of Ramachandran plot (%)	100
Residues in most favored regions of Ramachandran plot (%)	91.8
RMSD bond lengths (Å)	0.011
RMSD bond angles (°)	1.31
Mean B value (Å^2)	24.91
RMSD main chain B (Å^2)	1.019
Resolution range (Å)	14.9–1.6
R factor[c]	0.158
Free R factor[c]	0.192

[a] Value for the highest-resolution shell is given in parentheses.
[b] $R_{sym} = \Sigma(I - \langle I \rangle)/\Sigma I$. $\langle I \rangle$ is the average intensity over symmetry-equivalent reflections.
[c] R factor = $(\Sigma||F_{obs}| - |F_{calc}||)/\Sigma|F_{obs}|$, where the summations is over the working set of reflections. For the free R factor, the summation is over the test set of reflections (5% of the total reflections).

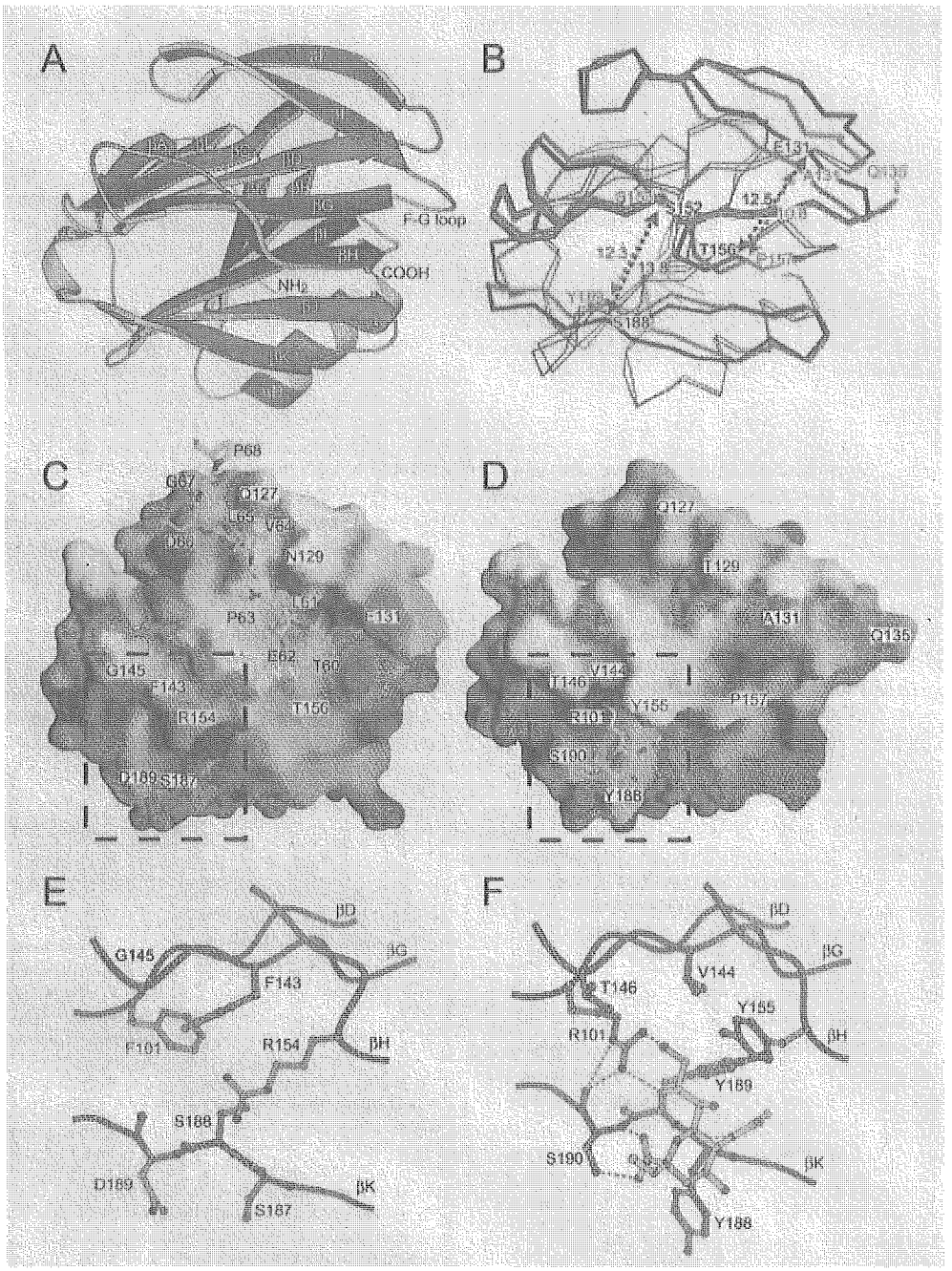

FIG. 3. Comparison of DS-1 and RRV VP8* cores. (A) Ribbon diagram of the DS-1 VP8* core. Labeling of secondary-structure elements is as previously described for the RRV VP8* core (14), except that strand βH, which splits into strands βH and βH′ in RRV, is continuous in DS-1. The EF β-hairpin is red, the six-stranded β-sheet is green, and the five-stranded β-sheet is blue. (B) Superimposed Cα traces of the DS-1 VP8* core (blue) and the RRV VP8* core (red). Residue Q135 of RRV, which lacks a structural equivalent in DS-1, is indicated. The blue and red arrows indicate the widths of surface clefts, measured in Å between Cα atoms of the labeled residues, for the DS-1 and RRV VP8* cores, respectively. (C) Surface representation of the DS-1 VP8* core colored by electrostatic potential. Blue is positive; red is negative. The bound leader of an adjacent molecule in the crystal is depicted with a ball-and-stick model. Residues in the space-filling model are labeled in white text boxes. Residues in the ball-and-stick model are labeled in yellow text boxes. (D) Surface representation of the RRV VP8* core colored by electrostatic potential. The bound sialoside is depicted with a ball-and-stick model. (E) Molecular details of the site in DS-1 VP8* that corresponds to the RRV SA binding pocket. The depicted area is indicated by the dashed outline in panel C. (F) Molecular details of the SA binding pocket of RRV VP8*. The depicted area is indicated by a dashed outline in panel D. Selected hydrogen bonds are indicated by dashed gray lines. In panels E and F, residues on strand βK are depicted with backbone and side chain atoms; only Cα and side chain atoms of other residues are shown. The perspective of all the panels is indicated by the arrow in Fig. 1.

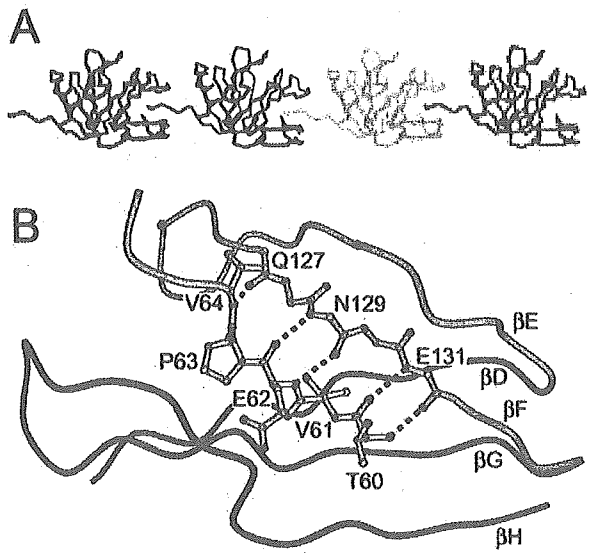

FIG. 4. Leader binding in the DS-1 VP8* core crystal. (A) Cα traces of representative molecules in the crystal. The cleft between the β-hairpin and the six-stranded β-sheet of each molecule binds the leader of an adjacent molecule. (B) Molecular details of the cleft-to-leader interaction. The leader is depicted in yellow. Hydrogen bonds are depicted as dotted black lines. Residues on strand βF are depicted without side chains. The perspective and coloring match Fig. 3A.

DS-1, the surface of the DS-1 VP8* core that corresponds to the RRV SA binding site is not an obvious binding pocket.

DS-1 VP8* binds a polypeptide chain in a second surface cleft. Does the DS-1 VP8* core structure suggest an alternative ligand to SA? The packing of the EF β-hairpin against the six-stranded β-sheet creates a cleft, which is adjacent to the cleft between the β-sheets that forms the SA binding pocket in RRV (Fig. 3A, C, and D). In the DS-1 VP8* core crystal, this cleft is occupied by the five N-terminal residues (residues 60 to 64) of an adjacent molecule, so that each DS-1 VP8* core "bites its neighbor's tail," linking the cores into chains (Fig. 4A). The bound N-terminal residues are not part of the tightly folded structure of the core, but instead form an extended N-terminal "leader." The equivalent residues are disordered in the RRV VP8* core crystal and solution structures (14). In the DS-1 VP8* core crystal, this leader is held in alignment by five backbone amide-to-carbonyl hydrogen bonds that form between residues 60, 62, and 64 of the leader and residues 131, 129, and 127 of strand F in the β-hairpin, thus making a new intermolecular three-stranded β-sheet with strands E and F (Fig. 4B). Leader binding is also stabilized by insertion of the aliphatic V61 side chain into a pocket lined by hydrophobic residues at the base of the cleft (Fig. 5B).

We used NMR spectroscopy to assay the binding in solution of a peptide based on the DS-1 VP8* core leader sequence to this potential peptide binding cleft (see Materials and Methods). The free peptide did not bind in the cleft with measurable affinity (data not shown). Close inspection of the DS-1 VP8* core crystal structure indicates that the bound leader does not fit the cleft optimally: the cleft continues beyond the N terminus of the bound leader (Fig. 3C), the hydrophobic pocket that holds the V61 side chain could accommodate a bulkier moiety (not shown), the P63 side chain prevents formation of potential hydrogen bonds between the leader and residues in strand H and the GH loop (Fig. 4B), and the leader is forced out of the cleft C terminal to P63 by steric hindrance from the tightly folded region of its own VP8* core (Fig. 4A).

The peptide binding cleft of the DS-1 core is one of the only exposed VP8* core surfaces that is conserved among SA-independent strains (Fig. 5B), suggesting a conserved function. A similar, but narrower, cleft is also present on the surface of the RRV VP8* core (Fig. 3D). Similar residues line this cleft in SA-dependent and SA-independent strains (see Table S1 in the supplemental material). Fitting to electron cryomicroscopy image reconstructions of virions from SA-dependent strains shows that this cleft is exposed at the tips of the VP4 spikes in a position favoring interaction with host cell proteins (Fig. 5B and D). As described previously, the VP8* β-hairpin appears to be an elaboration of a much shorter loop in the galectins, and it blocks the galectin carbohydrate binding site (14). The DS-1 VP8* core crystal structure suggests that this elaboration of the β-hairpin may also have created a new ligand binding site at the tip of the primed VP4 spike.

Structural polymorphism. Many rotavirus strains, such as DS-1, have a deletion in the FG loop (Table 3) so that they lack a residue that is structurally equivalent to RRV residue Q135 (Fig. 3B). The FG loop links the EF β-hairpin to the six-stranded β-sheet (Fig. 3A). Near the deletion, the potential peptide binding cleft between the EF β-hairpin and the six-stranded β-sheet is wider in the DS-1 VP8* core than in the RRV VP8* core (Fig. 3B), possibly because the shorter loop does not permit as close an approximation of the proximal portion of the β-hairpin to the six-stranded β-sheet.

Most human rotavirus strains have this deletion in the FG loop (Table 3). The infrequently isolated human rotavirus strains without the deletion have P types (such as 5A[3], 3[9], 4[10], and 11[14]), that also include animal rotavirus strains. These strains may have been introduced into human populations relatively recently. The deletion is consistently associated with SA independence (as verified by the presence of a hydrophobic residue at position 101), but it is not required for SA independence (Table 3). The phylogeny of rotavirus VP4 (6) does not clearly demonstrate whether this common structural feature is an adaptation to replication and spread in humans or simply a consequence of common ancestry: the clustering of VP4 molecules with the deletion in a single clade (containing P genotypes 4, 6, 8, and 19) is not absolute, and some bovine strains (in the outlying P[11] group) also have the deletion. Potential ligand binding in the cleft between the β-hairpin and the six-stranded β-sheet suggests that the structural polymorphism may reflect differences in ligand specificity.

Escape mutations selected by human neutralizing MAbs against rotavirus. Three human neutralizing MAbs against rotavirus have been derived from a phage display library of B-lymphocyte cDNA from naturally infected humans (21). The phage antibodies were selected for binding to rotavirus strain KU virions, tested for neutralization of strain KU, and converted to immunoglobulin G1 MAbs through recombinant DNA manipulation. One of the MAbs, 2-11G, binds VP7. The other two bind VP4 and neutralize heterotypically (i.e., neutralize more than one P type): 1-2H neutralizes P[4] and P[8]; 2-3E neutralizes P[6] and P[8].

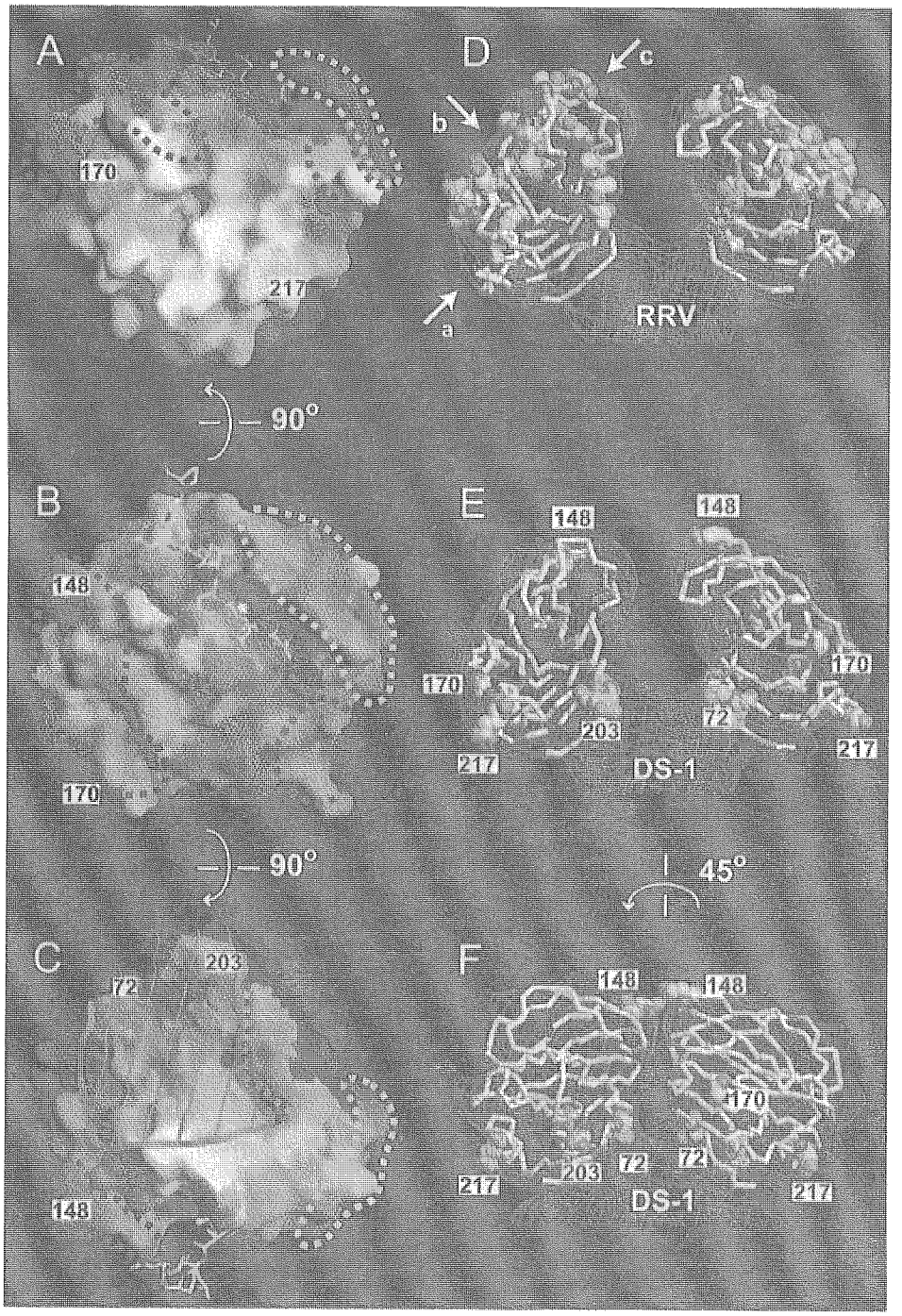

FIG. 5. Neutralization surfaces of the RRV and DS-1 VP8* cores. Panels A to C show three views of a surface representation of the DS-1 VP8* core, colored by conservation among a set of VP8* sequences that contains one representative from each of 14 SA-independent P genotypes (Table 3). Blue is conserved; red is variable. Residue numbers mark neutralization escape mutations selected in SA-independent human rotavirus strains. Dashed outlines mark the previously described (14) neutralization epitopes of SA-dependent strains: green, 8-1; blue, 8-2; yellow, 8-3; pink, 8-4. The white asterisk in panel B indicates a hydrophobic pocket at the base of the peptide binding cleft. Red lines in panel C mark a surface that is inaccessible to antibody binding when the DS-1 VP8* core is fitted to the head of the SA11-4F VP4 spike. The bound leader is depicted with a ball-and-stick model. The perspectives of panels A, B, and C are indicated by arrows a, b, and c, respectively, in panel D. An observer looking down arrow c would be "head down" to view the perspective in panel C. In panels D to F, Cα traces of VP8* cores are fitted to the molecular envelope of the head from an electron cryomicroscopy image reconstruction of the SA11-4F spike on primed virions. Residues selected in neutralization escape mutants are indicated with space-filling models. (D) The RRV VP8* core with escape mutations selected in SA-dependent animal rotavirus strains. (E) The DS-1 VP8* core with escape mutations selected in SA-independent human rotavirus strains. Exposed escape mutations are labeled by residue number. (F) The model from panel E rotated 45° to show more clearly the inaccessible escape mutations in the cleft between the heads.

TABLE 3. FG loop length correlations

Strain	Host	P type[a]	RRV Q135 equivalent[b]	SA dependence[c]	Residue at position 101	Genbank accession no.
SA11-4f	Simian	6[1]	Present	+	R	X57319
NCDV-Lin	Bovine	6[1]	Present	+[h]	R	M63267
RF	Bovine	6[1]	Present	+	R	U65924
BRV033	Bovine	6[1]	Present	+	R	U62155
SA11 cl3	Simian	5B[2]	Present	+[h]	R	M23188
RRV	Simian	5B[3]	Present	+[h]	R	AY033150
CU-1	Canine	5A[3]	Present	+	R	D13401
HCR3	Human	5A[3]	Present	+	R	L19712
K9	Canine	5A[3]	Present	+	R	D14725
Cat97	Feline	5A[3]	Present	+	R	D13402
DS-1	Human	1B[4]	Absent	−[h]	F	DQ141310
L26	Human	1B[4]	Absent	−	F	M58292
4S	Porcine	7[5]	Present	−	R	L10358
UK	Bovine	7[5]	Present	−[d,h]	R	M22306
WC3	Bovine	7[5]	Present	−	R	AY050271
B461	Bovine	7[5]	Present	−	R	M63267
678	Bovine	7[5]	Present	−	R	D32054
M37	Human	2A[6]	Absent	−	I	None[e]
1076	Human	2A[6]	Absent	−[h]	I	None[e]
McN13	Human	2A[6]	Absent	−	I	None[e]
ST3	Human	2A[6]	Absent	−	I	L33895
Gott	Porcine	2B[6]	Absent	−	V	M33516
CRW-8	Porcine	9[7]	Present	+	R	L07888
OSU	Porcine	9[7]	Present	+[h]	R	X13190
H1	Equine	9[7]	Present	+	R	D16341
TFR-41	Porcine	9[7]	Present	+	R	L07889
YM	Porcine	9[7]	Present	+	R	M63231
Wa	Human	1A[8]	Absent	−	F	M96825
KU	Human	1A[8]	Absent	−[h]	F	M21014
MO	Human	1A[8]	Absent	−	F	AB008278
YO	Human	1A[8]	Absent	−	F	AB008279
Ito	Human	1A[8]	Absent	−	F	AB008280
VA70	Human	1A[8]	Absent	−	F	AJ540229
Hochi	Human	1A[8]	Absent	−	F	AB039943
K8	Human	3[9]	Present	−[h]	R	D90260
O264	Human	3[9]	Present	−	R	AB008665
Cat2	Feline	3[9]	Present	−	R	D13403
69M	Human	4[10]	Present	−[h]	R	M60600
B233	Bovine	8[11]	Absent	−[h]	F	D13394
I321	Human	8[11]	Absent	−	F	L07657
H-2	Equine	4[12]	Present	−[h]	R	L04638
FI-14	Equine	4[12]	Present	−	R	D13398
FI23	Equine	4[12]	Present	−	R	D16342
A46	Porcine	[13]	Present	−[h]	M	AY070274
Ala	Lapine	11[14]	Present	−[h]	R	U62149
C-11	Lapine	11[14]	Present	−	R	U62150
BAP-2	Lapine	11[14]	Present	−	R	U62151
R-2	Lapine	11[14]	Present	−	R	U62152
PA169	Lapine	11[14]	Present	−	R	D14724
HAL1166	Human	11[14]	Present	−	R	L20885
Mc35	Human	11[14]	Present	−	R	D14032
Lp14	Ovine	[15]	Present	−[h]	R	L11599
EW	Murine	10[16]	Present	−	R	U08429
EC	Murine	10[16]	Present	+/−[f]	R	U08421
EB	Murine	10[16]	Present	−[h]	R	U08419
EDIM	Murine	10[16]	Present	−	R	AF039219
Ty-1	Avian	[17]	Present	−[h]	R	L41493
L338	Equine	12[18]	Present	+/−[f]	R	D13399
4F	Porcine	[19]	Absent	−[h]	V	L10359
EHP	Murine	[20]	Present	+/−[g]	R	U08424

[a] P serotype[P genotype]. Some strains have not been serotyped. Many of the strain classifications were obtained from reference 6.
[b] Indicates the presence or absence of a residue that is structurally equivalent to residue 135 of strain RRV.
[c] SA dependence is based on published data that define SA independence as a preserved infectious titer on cultured cells or enterocytes digested with *Arthrobacter ureafaciens* neuraminidase (5, 6, 10, 31).
[d] Although UK entry is not SA dependent, it binds glycosphingolipids with a specificity dependent upon the SA moiety in the oligosaccharide chain (10).
[e] Sequences from reference 17.
[f] Weak inhibition by neuraminidase digestion of MA104 cells (6).
[g] Cell-type-specific neuraminidase sensitivity (31).
[h] Strain included in the SA-dependent and SA-independent sets used to calculate variability for Table S1 in the supplemental material and Fig. 5A to C.

TABLE 4. Neutralization escape mutations selected by MAbs that recognize VP8* of human rotavirus strains

MAb	Escape mutation (strain)[a]	Immunization regimen	P genotypes neutralized (not neutralized)[b]	Immunized species	Initial screen	Reference
1-2H	G170D (KU)	Natural infection	P[4, 8] (P[5, 6, 9, 10])	Human	Binding	21
2-3E	E203K (KU)	Natural infection	P[6, 8] (P[4, 5, 9, 10])	Human	Binding	21
HS6	T721 (ST3)	IP[c] with ST3	P[6, +/−8][d] (P[4])	Mouse	Neutralization	35
HS11	E217K (ST3)	IP with ST3	P[6] (P[4, 8])	Mouse	Neutralization	35
RV-5:2	Q148R (RV-5)	IP and IV[e] with RV-5	P[4] (P[2, 3, 5, 6, 8, 10])	Mouse	Neutralization	8

[a] P genotypes of rotavirus strains: KU, P[8]; ST3, P[6]; RV-5, P[4].
[b] Only listed P genotypes were tested.
[c] IP, intraperitoneal hyperimmunization.
[d] Some, but not all, P[8] strains are neutralized.
[e] IV, intravenous hyperimmunization.

We have mapped the residues recognized by 1-2H and 2-3E in strain KU, using neutralization escape mutant analysis (Table 4). MAb 1-2H selects a unique G-to-D mutation at VP4 residue 170 (virus strain m-KU-1-2H), and MAb 2-3E selects a unique E-to-K mutation at VP4 residue 203 (virus strain m-KU-2-3E). Both mutations are in the VP8* fragment of VP4. Three other VP8*-specific antibodies that neutralize human strains of rotavirus have been described (26, 35, 36). Two of these MAbs, HS11 and RV5:2, neutralize homotypically, but the other MAb, HS6, neutralizes P[6] and some P[8] viruses (Table 4). Thus, three of five neutralizing monoclonal antibodies that recognize VP8* of human rotavirus strains are heterotypic in their neutralization specificities. A more limited degree of heterotypic neutralization has been observed among the 20 mapped MAbs that bind VP8* and neutralize animal rotavirus strains (see Table S2 in the supplemental material). Heterotypic neutralization by monoclonal antibodies derived from naturally infected humans may reflect selection for heterotypic antibodies by repeated rotavirus infection. This result correlates well with the increasingly broad serum neutralizing response against rotavirus elicited by reinfection with rotaviruses of the same or different rotavirus serotypes (19, 43).

Although VP5* is more conserved among strains than is VP8*, the presence of heterotypic neutralization epitopes on VP8* of human strains suggests that immunization with recombinant VP8* of human strains could induce a heterotypic neutralizing antibody response. Such a response has been demonstrated against VP8* from an animal rotavirus strain, as primary immunization of laboratory animals with recombinant VP8* of the simian strain RRV does produce heterotypically neutralizing antibodies (16).

Mapping of neutralization escape mutations on the DS-1 VP8* core structure. As previously described, the 20 neutralization escape mutations mapped to VP8* of SA-dependent animal rotavirus strains cluster in four epitopes (14). The five neutralization escape mutations now mapped to VP8* of SA-independent human rotavirus strains do not cluster in these epitopes or in any easily identifiable new epitopes (Fig. 5A to C, labeled residues). Only the mutation at residue 148 of human strain RV-5 lies within one of the previously described epitopes (designated 8-1). Because the DS-1 and RRV VP8* cores have a common fold, gross structural differences do not explain the distinct distributions of escape mutations.

When the RRV VP8* core crystal structure is fitted to the spike envelope of a 12-Å-resolution electron cryomicroscopy image reconstruction of trypsin-primed, SA-dependent rotavirus particles, all of the escape mutations on VP8* of SA-dependent strains are accessible for antibody binding, forming "caps" at the tips of the spikes' heads (Fig. 5D). Although the DS-1 VP8* core fits the same molecular envelope, the escape mutations of SA-independent human strains are not in the most accessible locations, and three (at residues 72, 203, and 217) ring the base of the head (Fig. 5E and F). In fact, the escape mutation at residue 72 contributes to the point of attachment of head to body and to the surface of the gap between the paired heads, where it is not accessible for antibody binding (Fig. 5C, E, and F). The escape mutation at residue 203 also contributes to the surface of the gap between head and body and is on the boundary between accessible and inaccessible surfaces.

Thus, the distribution of escape mutations suggests that the state of the VP4 spike recognized by some VP8*-specific antibodies that neutralize SA-independent human rotavirus strains differs from the state recognized by VP8*-specific antibodies that neutralize SA-dependent animal rotavirus strains. Alternatively, the selected residues could mediate escape from neutralization by indirect steric effects, rather than by direct disruption of an epitope. No electron cryomicroscopy image reconstructions of SA-independent rotavirus virions are currently available to test the hypothesis that the conformations of trypsin-primed spikes on SA-independent and SA-dependent strains expose different molecular surfaces of the VP8* core for potential antibody binding.

VP4 spikes have multiple conformations during rotavirus entry. Prior to trypsin priming, the spikes are flexible and therefore not visible in averaged icosahedral image reconstructions (9). Trypsin priming rigidifies pairs of VP4 molecules to produce spikes. Threefold symmetry of the portion of VP4 buried under the VP7 shell (44), the trimeric appearance of altered VP4 spikes on virions that have been treated with alkali (39), and the stable trimer formed by a rearranged VP5* fragment (13) suggest that each VP4 cluster on the virion surface may contain three molecules, one of which remains flexible after trypsin priming. In addition, electron cryomicroscopy image reconstructions demonstrate subtle conformational differences in spike morphology among SA-dependent rotavirus strains (38). The 22- to 23-Å resolution limit of these reconstructions does not permit a precise determination of the boundaries of the accessible surfaces on the variants. Thus, either strain differences in spike morphology or the multiple conformational states of VP4 could explain the distribution of

neutralization escape mutations on VP8* of human rotavirus strains.

In summary, although the VP8* cores of an SA-dependent strain (RRV) and of an SA-independent strain (DS-1) are substantially similar, there are significant structural differences between the two phenotypic variants. The biochemical characteristics of both variants, including ease of expression and purification, high solubility, and chemical stability make them promising components for a potential second-generation recombinant rotavirus vaccine. In this regard, heterotypic neutralization by MAbs recognizing VP8* of human strains is a particularly promising finding. Differences between the RRV and DS-1 VP8* cores in the region that corresponds to the RRV SA binding site make it unlikely that DS-1 VP8* binds an alternative carbohydrate ligand in this location. A widened cleft between the EF β-hairpin and the six-stranded β-sheet in the DS-1 VP8* core and the binding of a peptide chain in this cleft suggest that VP8* may bind a protein ligand. The very different neutralization surfaces of SA-dependent and SA-independent viruses suggest different mechanisms of neutralization and, possibly, differences in spike morphology. Further structural studies of SA-independent rotavirus strains could reveal differences in the VP4 spike that are directly relevant to the pathogenesis of rotavirus gastroenteritis in children.

ACKNOWLEDGMENTS

We thank Marina Babyonyshev for technical assistance, Mary Estes and Mario Gorziglia for recombinant baculoviruses containing cloned KU and DS-1 genes, Eric Vogan for assistance in analyzing X-ray diffraction data, Gerhard Wagner for use of NMR spectrometers, Stephen C. Harrison for scientific advice and support, the MACCHESS staff at the Cornell High Energy Synchrotron Source for assistance with data collection, the Harvard Medical School Biopolymers Facility for DNA sequencing and oligonucleotide synthesis, and Michael Berne and the Tufts Protein Chemistry Facility for mass spectrometry, N-terminal sequencing, and peptide synthesis. We acknowledge the use of electron cryomicroscopy facilities at the National Center for Macromolecular Imaging, funded by NIH, at Baylor College of Medicine.

This work was supported by NIH grant R37 AI 36040 to B.V.V.P. and by NIH grant R01 AI 053174 and an Ellison Medical Foundation New Scholars in Global Infectious Disease Award to P.R.D.

REFERENCES

1. **Bartels, C., T.-H. Xia, M. Billeter, P. Guntert, and K. Wuthrich.** 1995. The program XEASY for computer-supported NMR spectral analysis of biological macromolecules. J. Biomol. NMR **5**:1–10.
2. **Bastardo, J. W., and I. H. Holmes.** 1980. Attachment of SA-11 rotavirus to erythrocyte receptors. Infect. Immun. **29**:1134–1140.
3. **Brunger, A. T., P. D. Adams, G. M. Clore, W. L. DeLano, P. Gros, R. W. Grosse-Kunstleve, J. S. Jiang, J. Kuszewski, M. Nilges, N. S. Pannu, R. J. Read, L. M. Rice, T. Simonson, and G. L. Warren.** 1998. Crystallography and NMR system: a new software suite for macromolecular structure determination. Acta Crystallogr. D **54**:905–921.
4. **Ciarlet, M., S. E. Crawford, and M. K. Estes.** 2001. Differential infection of polarized epithelial cell lines by sialic acid-dependent and sialic acid-independent rotavirus strains. J. Virol. **75**:11834–11850.
5. **Ciarlet, M., and M. K. Estes.** 1999. Human and most animal rotavirus strains do not require the presence of sialic acid on the cell surface for efficient infectivity. J. Gen. Virol. **80**:943–948.
6. **Ciarlet, M., J. E. Ludert, M. Iturriza-Gomara, F. Liprandi, J. J. Gray, U. Desselberger, and M. K. Estes.** 2002. The initial interaction of rotavirus strains with *N*-acetyl-neuraminic (sialic) acid residues on the cell surface correlates with VP4 genotype, not species of origin. J. Virol. **76**:4087–4095.
7. **Collaborative Computational Project.** 1994. The CCP4 suite: programs for protein crystallography. Acta Crystallogr. D **50**:760–763.
8. **Coulson, B. S., J. M. Tursi, W. J. McAdam, and R. F. Bishop.** 1986. Derivation of neutralizing monoclonal antibodies to human rotaviruses and evidence that an immunodominant neutralization site is shared between serotypes 1 and 3. Virology **154**:302–312.
9. **Crawford, S. E., S. K. Mukherjee, M. K. Estes, J. A. Lawton, A. L. Shaw, R. F. Ramig, and B. V. Prasad.** 2001. Trypsin cleavage stabilizes the rotavirus VP4 spike. J. Virol. **75**:6052–6061.
10. **Delorme, C., H. Brussow, J. Sidoti, N. Roche, K. A. Karlsson, J. R. Neeser, and S. Teneberg.** 2001. Glycosphingolipid binding specificities of rotavirus: identification of a sialic acid-binding epitope. J. Virol. **75**:2276–2287.
11. **Desselberger, U., M. Iturriza-Gomara, and J. J. Gray.** 2001. Rotavirus epidemiology and surveillance. Novartis Found. Symp. **238**:125–152.
12. **Dormitzer, P. R., H. B. Greenberg, and S. C. Harrison.** 2001. Proteolysis of monomeric recombinant rotavirus VP4 yields an oligomeric VP5* core. J. Virol. **75**:7339–7350.
13. **Dormitzer, P. R., E. B. Nason, B. V. Prasad, and S. C. Harrison.** 2004. Structural rearrangements in the membrane penetration protein of a non-enveloped virus. Nature **430**:1053–1058.
14. **Dormitzer, P. R., Z.-Y. J. Sun, G. Wagner, and S. C. Harrison.** 2002. The rhesus rotavirus VP4 sialic acid binding domain has a galectin fold with a novel carbohydrate binding site. EMBO J. **21**:885–897.
15. **Estes, M. K., D. Y. Graham, and B. B. Mason.** 1981. Proteolytic enhancement of rotavirus infectivity: molecular mechanisms. J. Virol. **39**:879–888.
16. **Fiore, L., H. B. Greenberg, and E. R. Mackow.** 1991. The VP8 fragment of VP4 is the rhesus rotavirus hemagglutinin. Virology **181**:553–563.
17. **Gorziglia, M., K. Green, K. Nishikawa, K. Taniguchi, R. Jones, A. Z. Kapikian, and R. M. Chanock.** 1988. Sequence of the fourth gene of human rotaviruses recovered from asymptomatic or symptomatic infections. J. Virol. **62**:2978–2984.
18. **Gorziglia, M., G. Larralde, A. Z. Kapikian, and R. M. Chanock.** 1990. Antigenic relationships among human rotaviruses as determined by outer capsid protein VP4. Proc. Natl. Acad. Sci. USA **87**:7155–7159.
19. **Green, K. Y., K. Taniguchi, E. R. Mackow, and A. Z. Kapikian.** 1990. Homotypic and heterotypic epitope-specific antibody responses in adult and infant rotavirus vaccinees: implications for vaccine development. J. Infect. Dis. **161**:667–679.
20. **Guntert, P., V. Dotsch, G. Wider, and K. Wuthrich.** 1992. Processing of multi-dimensional NMR data with the new software PROSA. J. Biomol. NMR **2**:619–629.
21. **Higo-Moriguchi, K., Y. Akahori, Y. Iba, Y. Kurosawa, and K. Taniguchi.** 2004. Isolation of human monoclonal antibodies that neutralize human rotavirus. J. Virol. **78**:3325–3332.
22. **Hoshino, Y., and A. Z. Kapikian.** 1996. Classification of rotavirus VP4 and VP7 serotypes. Arch. Virol. Suppl. **12**:99–111.
23. **Jeffrey, P. D., J. Bajorath, C. Y. Chang, D. Yelton, I. Hellstrom, K. E. Hellstrom, and S. Sheriff.** 1995. The X-ray structure of an anti-tumour antibody in complex with antigen. Nat. Struct. Biol. **2**:466–471.
24. **Jones, T. A., J. Y. Zou, S. W. Cowan, and M. Kjeldgaard.** 1991. Improved methods for building protein models in electron density maps and the location of errors in these models. Acta Crystallogr. A **47**:110–119.
25. **Kapikian, A. Z., Y. Hoshino, and R. M. Chanock.** 2001. Rotaviruses, p. 1787–1833. *In* D. M. Knipe, P. M. Howley, D. D. Griffin, R. A. Lamb, M. A. Martin, B. Roizman, and S. E. Straus (ed.), Fields virology, 4th ed., vol. 2. Lippincott Williams and Wilkins, Philadelphia, Pa.
26. **Kirkwood, C. D., R. F. Bishop, and B. S. Coulson.** 1996. Human rotavirus VP4 contains strain-specific, serotype-specific and cross-reactive neutralization sites. Arch. Virol. **141**:587–600.
27. **Kraulis, J.** 1991. MOLSCRIPT: a program to produce both detailed and schematic plots of protein structures. J. Appl. Crystallogr. **24**:946–950.
28. **LaMonica, R., S. S. Kocer, J. Nazarova, W. Dowling, E. Geimonen, R. D. Shaw, and E. R. Mackow.** 2001. VP4 differentially regulates TRAF2 signaling, disengaging JNK activation while directing NF-kappa B to effect rotavirus-specific cellular responses. J. Biol. Chem. **276**:19889–19896.
29. **Laskowski, R. A., M. W. MacArthur, D. S. Moss, and J. M. Thornton.** 1993. PROCHECK: a program to check the sterochemical quality of protein structures. J. Appl. Crystallogr. **26**:283–291.
30. **Livingstone, C. D., and G. J. Barton.** 1993. Protein sequence alignments: a strategy for the hierarchical analysis of residue conservation. Comput. Appl. Biosci. **9**:745–756.
31. **Ludert, J. E., B. B. Mason, J. Angel, B. Tang, Y. Hoshino, N. Feng, P. T. Vo, E. M. Mackow, F. M. Ruggeri, and H. B. Greenberg.** 1998. Identification of mutations in the rotavirus protein VP4 that alter sialic-acid-dependent infection. J. Gen. Virol. **79**:725–729.
32. **Mackow, E. R., R. D. Shaw, S. M. Matsui, P. T. Vo, M. N. Dang, and H. B. Greenberg.** 1988. The rhesus rotavirus gene encoding protein VP3: location of amino acids involved in homologous and heterologous rotavirus neutralization and identification of a putative fusion region. Proc. Natl. Acad. Sci. USA **85**:645–649.
33. **Matsui, S. M., P. A. Offit, P. T. Vo, E. R. Mackow, D. A. Benfield, R. D. Shaw, L. Padilla-Noriega, and H. B. Greenberg.** 1989. Passive protection against rotavirus-induced diarrhea by monoclonal antibodies to the heterotypic neutralization domain of VP7 and the VP8 fragment of VP4. J. Clin. Microbiol. **27**:780–782.
34. **Nicholls, A., K. A. Sharp, and B. Honig.** 1991. Protein folding and association: insights from interfacial and thermodynamic properties of hydrocarbons. Proteins **11**:281–296.

35. **Padilla-Noriega, L., S. J. Dunn, S. Lopez, H. B. Greenberg, and C. F. Arias.** 1995. Identification of two independent neutralization domains on the VP4 trypsin cleavage products VP5* and VP8* of human rotavirus ST3. Virology **206:**148–154.
36. **Padilla-Noriega, L., R. Werner-Eckert, E. R. Mackow, M. Gorziglia, G. Larralde, K. Taniguchi, and H. B. Greenberg.** 1993. Serologic analysis of human rotavirus serotypes P1A and P2 by using monoclonal antibodies. J. Clin. Microbiol. **31:**622–628.
37. **Parashar, U. D., E. G. Hummelman, J. S. Bresee, M. A. Miller, and R. I. Glass.** 2003. Global illness and deaths caused by rotavirus disease in children. Emerg. Infect. Dis. **9:**565–572.
38. **Pesavento, J. B., A. M. Billingsley, E. J. Roberts, R. F. Ramig, and B. V. Prasad.** 2003. Structures of rotavirus reassortants demonstrate correlation of altered conformation of the VP4 spike and expression of unexpected VP4-associated phenotypes. J. Virol. **77:**3291–3296.
39. **Pesavento, J. B., S. E. Crawford, E. Roberts, M. K. Estes, and B. V. Prasad.** 2005. pH-induced conformational change of the rotavirus VP4 spike: implications for cell entry and antibody neutralization. J. Virol. **79:**8572–8580.
40. **Sato, K., Y. Inaba, T. Shinozaki, R. Fujii, and M. Matumoto.** 1981. Isolation of human rotavirus in cell cultures: brief report. Arch. Virol. **69:**155–160.
41. **Shaw, A. L., R. Rothnagel, D. Chen, R. F. Ramig, W. Chiu, and B. V. Prasad.** 1993. Three-dimensional visualization of the rotavirus hemagglutinin structure. Cell **74:**693–701.
42. **Ward, R. L., D. R. Knowlton, and M. J. Pierce.** 1984. Efficiency of human rotavirus propagation in cell culture. J. Clin. Microbiol. **19:**748–753.
43. **Ward, R. L., D. S. Sander, G. M. Schiff, and D. I. Bernstein.** 1990. Effect of vaccination on serotype-specific antibody responses in infants administered WC3 bovine rotavirus before or after a natural rotavirus infection. J. Infect. Dis. **162:**1298–1303.
44. **Yeager, M., J. A. Berriman, T. S. Baker, and A. R. Bellamy.** 1994. Three-dimensional structure of the rotavirus haemagglutinin VP4 by cryo-electron microscopy and difference map analysis. EMBO J. **13:**1011–1018.
45. **Zhou, Y. J., J. W. Burns, Y. Morita, T. Tanaka, and M. K. Estes.** 1994. Localization of rotavirus VP4 neutralization epitopes involved in antibody-induced conformational changes of virus structure. J. Virol. **68:**3955–3964.